Cargese 2017: Liouville field theory and log-REM models

Raoul Santachiara

Université Paris-Saclay, Laboratoire de Physique Théorique et Modèles Statistiques

Abstract: These lectures are based on the work 1611.02193 done in collaboration with **Xiangyu Cao**, **Pierre Le Doussal** and **Alberto Rosso**. I would like to thank specially Xiangyu, who has been the main actor behind the results mentioned here. The following notes, meant to be an expanded version of what is said during the lectures, have been taken from Xiangyu's Phd thesis: 1705.06896. Here a more complete and satisfying presentation of the following results can be found. Finally I thank **Sylvain Ribault** that has introduced me to the conformal bootrap approach to Liouville theory

Contents

1 Introduction

In these two lectures, we will discuss the LFT/log-REM connection and argue that it provides not only a statistical interpretation of subtle (and somehow unexplored) properties of the LFT, but also a route to calculate certain lower order corrections without using the replica approach.

Log-correlated Random Energy Models (log-REM) are a class of disordered statistical models that display a glassy behavior generated by the competition between deep metastable states and thermal excitations. Together with the REM models, this is the simplest class of models that i) have a second-order phase transition separating a entropy (high-temperature) dominating phase from an energy-fluctuations phase (-low-temperature), ii) in a replica approach, this phase transition can be described by a one step replica symmetry breaking (1RSB).

We have seen the definition and the solution of the Liouville field theory (LFT) theory in the lectures of Sylvain Ribault. There the LFT is introduced as a solution of a CFT conformal bootrap approach. Here we will define LFT via a lagrangian formulation. A nice review can be found in the last year Cargese course [1] (which actually has been inspiring for our results).

An exact mapping is established between the $c \geq 25$ Liouville field theory (LFT) and the Gibbs measure statistics of a thermal particle in a 2D Gaussian Free Field plus a logarithmic confining potential [2]. More precisely, correlation functions of LFT describe naturally the correlation functions of the *Gibbs measure* of these log-REM, *i.e.*, LFT describes the *positions* of thermal particles in 2D GFF–random potential.

This link was observed for the first time by Kogan, Mudry and Tsvelik [3], Le-Doussal, Carpentier [9]. However, at their time, this insight did not lead to precise predictions on log-REM by the LFT, because of three difficulties:

1. The thermodynamics of the log-REM was not yet developed. By now, this difficulty is sufficiently resolved.

2. The authors of [3] investigated the mapping on the *infinite* plane, which is the most tricky case.

The highlight will be the numerical test of an exact prediction, eq. (5.32), which equates the disorder–averaged Gibbs measure of a 2D log-REM and a LFT *four–point* correlation function. We emphasize "four–point" because in general, a CFT is completely solved if and only if we can calculate its four–point functions. So, remarkably, the simplest log-REM application involves all the field–theory features of LFT. We obtained explicit results on the probability distribution of the position of the minimum a 2DGFF. To obtain this we combined the conformal bootstrap and one-step replica symmetry breaking methods.

Another major consequence is that the Liouville OPE, which determines the short–distance of its correlation function, provides new predictions about *universal features* of log-REM. In particular they predict the corrections to multi-fractal exponent as well as to the overlap distributions. This will unveil important statistical significations of the subtle

structure of the Liouville OPE: the presence/absence of the so-called *discrete terms*. This LFT feature was sketched already in [4], and elaborated in more recent works [5–8].

Below we tried to resume in a picture the general logic behind the work we are presenting:

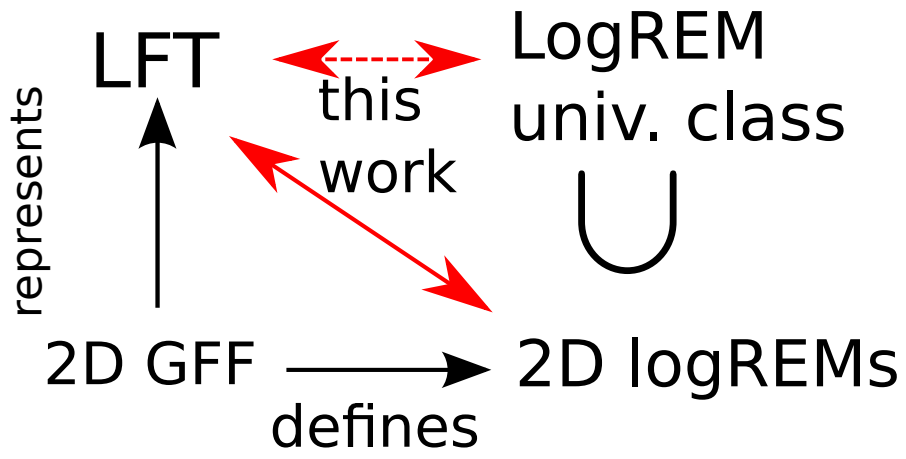

2 Freezing transitions in (log-) Random Energy Models

2.1 Thermal particle on a short- vs long- range correlated random potential

We consider the statistical physics of a particle in a random potential V_j where j denotes on of the M points of a $d-$dimensional lattice:

$$\mathcal{Z} = \sum_{j=1}^{M} \exp\left(-\beta V_j\right), \quad \mathcal{F} = -\beta^{-1} \ln \mathcal{Z} \tag{2.1}$$

Note that the partition function and the free-energy $\mathcal{Z}$ and $\mathcal{F}$ are random numbers.

Let us consider Gaussian potentials on a one-dimensional lattice, labelled by $j = 0, \dots, M-1$, with periodic boundary condition. The potential can be generated by Fourier transform:

$$V_j = \Re \sum_{k=-M/2}^{M/2-1} \sqrt{\mu_k} \exp\left(2\pi \mathbf{i} \frac{jk}{M}\right) \mathsf{N}_k \,. \tag{2.2}$$

Here, (N_k) is a sequence of *iid* standard complex Gaussian variables. $\mu_k \geq 0$ control all the statistical properties of the potential, *e.g.*, the variance and the correlations:

$$\begin{aligned} \overline{V_j^2} &= \sum_{k=-M/2}^{M/2-1} \mu_k \,, \; \overline{V_0 V_j} = \sum_{k=-M/2}^{M/2-1} \mu_k \cos\left(\pi \frac{jk}{M}\right) \,, \\ \overline{(V_0 - V_j)^2} &= \sum_{k=-M/2}^{M/2-1} 4\mu_k \sin^2\left(\pi \frac{jk}{M}\right) \,, \end{aligned} \tag{2.3}$$

The trivial global shift $\mu_{k=0}$ will be set to 0.
Let's consider the class of potential defined by:

$$\mu_0 = 0 \,, \; \mu_{k\neq 0} = \pi M^{-1} \sin^{-\alpha}\left(\frac{\pi\,|k|}{M}\right) \overset{|k|<<M}{\sim} k^{-\alpha} M^{\alpha-1} \,. \tag{2.4}$$

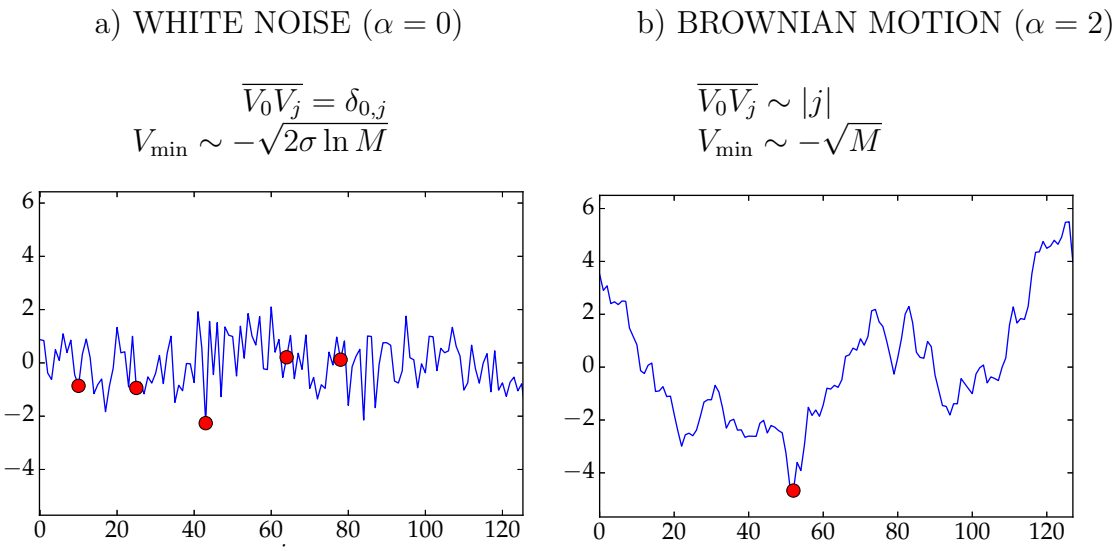

Figure 1. Samples of random potentials defined by eq. (2.2) and (2.4), with $\alpha = 0$ (white noise, left panel) and $\alpha = 2$ (Brownian motion, right panel). In the a) case, a thermal particle visits freely the whole system, while in the b) case, it is confined in the deepest minimum.

where α is a real parameter. Sample of these potential for $\alpha = 0, 2$ are shown in Fig 1.

A standard strategy of qualitatively understanding the behavior of the free energy (2.1) is to compare the minimum energy, $V_{\min} = \min_{i=0}^{M-1}(V_i)$, with the entropy of visiting every one of the M sites $S = \ln M$. This determines roughly whether the system is in an energy-dominating, or entropy-dominating, phase. Such an analysis was carried out in detail in [9], section II.

- When $\alpha < 1$, $|V_{\min}| << \ln M$. The model has only a high-T phase;
- When $\alpha > 1$, $|V_{\min}| \sim M^{(\alpha-1)/2} \gg \ln M$. The model has only a low-T phase.

2.2 1D Log-REM: existence of a freezing transition

When $\alpha = 1$ is in fact the most interesting from the thermodynamic point of view. This is our first example of (a 1d) log-REM and a sample of the potential is shown in Fig(2.2).

$$\overline{V_j V_0} \sim 2 \ln(M/|j|) \,, \; 1 << j << M \,. \tag{2.5}$$

The variance $\overline{V_j^2} = 2 \ln M + O(1)$, *i.e.*, it is proportional to the (infinite-T) entropy $S = \ln M$, comparable to the REM. Therefore, the out-come of energy–entropy competition depends non–trivially on the temperature and induce a phase transition at some finite $\beta = \beta_c$ separating a high-T phase from a low-T phase.

The first dominant terms of the free energy for the log-REM are:

$$\mathcal{F} \to \begin{cases} -(\beta + \beta^{-1}) \ln M + f \,, & \beta < 1 \,, \\ -2 \ln M - \frac{1}{2} \ln \ln M + f \,, & \beta = 1 \\ -2 \ln M - \frac{3}{2} \ln \ln M + f \,, & \beta > 1 \,. \end{cases} \tag{2.6}$$

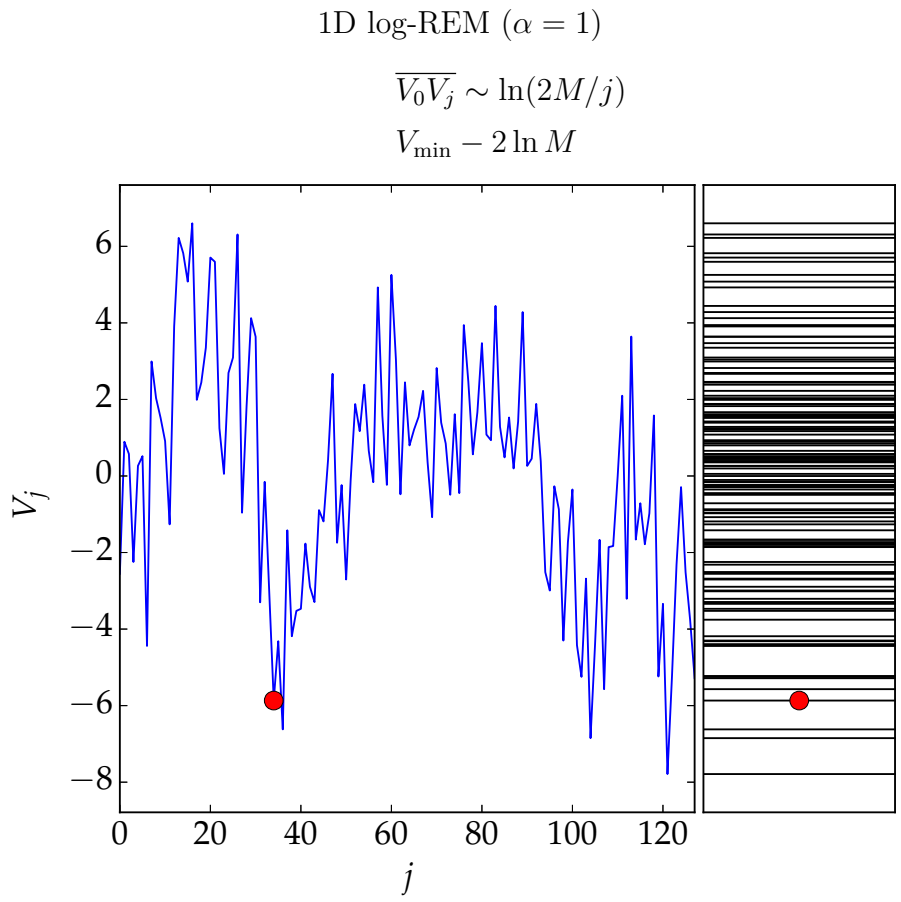

Figure 2. A sample of the log-correlated random potential, generated by eq. (2.2) and (2.4), with $\alpha = 1$. The potential is plotted in the left panel; all its energy values are plotted at the right panel. A thermal particle at finite temperature occupying a position with low–lying energy (but not the minimum energy, which is attained at $j = 120$) is also depicted.

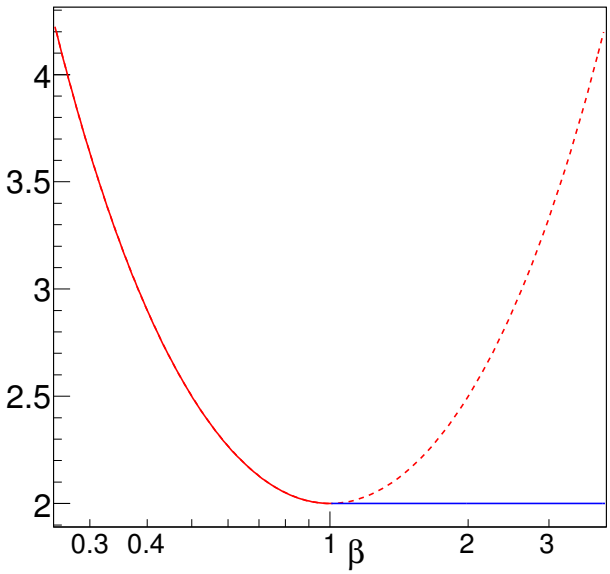

Note that the subsub leading terms $f \sim O(1)$) are random and described by certain PDF $P(f)$. These are in general difficult to compute and depend on the details of the

model (for instance the geometry on which are defined). We derived later, using the replica approach and the so-called freezing scenarion the PDF of f for the log-REM considered here (we recall, defined by taking $\alpha = 1$ in (2.4)). The $3/2 \ln \ln M$ corrections as well as the $|f|e^f$ left tail ($f \to -\infty$) of the distribution $P(f)$ are universal for all log-REM.

2.3 2d log-REM models from dicrete GFF

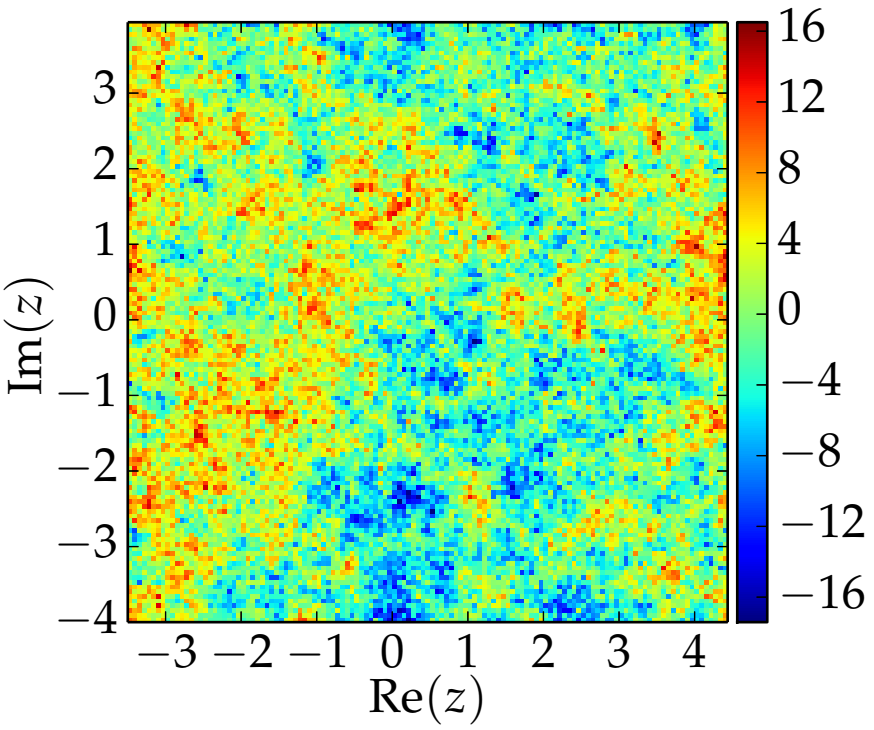

Figure 3. A sample of the 2D GFF, regularized on a lattice on a square torus (periodic boundary condition), with $M = 2^{16}$; the image is compressed so there are less visible pixels.

We can easily define a log-REM model in d=2 dimension by taking a toroidal square lattice of size $R \times R$ and of lattice spacing ϵ, such that $L = R/\epsilon$ and $M = L^2 = R^2/\epsilon^2$. Then the field can be generated by a 2D analogue of eq. (2.2)

$$\phi(x + \mathbf{i}y) = \Re \sum_{q=-L/2}^{L/2-1} \sum_{p=-L/2}^{L/2-1} \exp\left[2\pi \mathbf{i} \left(\frac{qx}{L} + \frac{py}{L}\right)\right] \mathsf{N}_{p,q} \sqrt{\mu_{p,q}}\,, \tag{2.7}$$

$$\mu_{p,q} = \frac{2}{\pi(p^2+q^2)}\,,\ \mu_{0,0} = 0\,. \tag{2.8}$$

A sample is plotted in Figure 3. The covariance of such a field is

$$\overline{\phi(z)\phi(w)} = 4 \ln \left|\frac{R}{z-w}\right|\,, \epsilon << |z-w| << R\,, \tag{2.9}$$

$$\overline{\phi(z)^2} = 2 \ln M + O(1) \tag{2.10}$$

Now that we have generated a discrete potential, the discrete partition function $\mathcal{Z}$ eq. (2.1) is defined by setting $V_j = \phi(x_j + \mathbf{i}y_j)$. The thermodynamic limit is achieved by taking $M \to \infty$.

The particle goes through also a freezing transition as the free-energy ahs the same leading and sub-leading behavior as in (2.6).

The model (2.7) is the lattice version of a a thermal particle in a 2D GFF potential. We will compare results of the LFT theory with the statistical data generated by (2.7).

2.4 Freezing transition in the Random Energy Model (REM)

The log-REM models shares the main physical features (the existence of a freezing phase transition where the symmetry replica is broken...) with a simpler model, the REM model where the disorder is not correlated:

$$P(V_j) = \frac{1}{\sqrt{4\pi \ln M}} \exp\left(-\frac{V_j^2}{4 \ln M}\right), \quad \overline{V_i V_j} = 2 \ln M \delta_{i,j} \tag{2.11}$$

We use the REM to show the physics of these disordered model in a more quantitative way.

2.5 Free-energy leading term and existence of transition

Following [10], we consider the micro–canonical ensemble. For this, let us fix an energy E. Since the energies are independent, $\mathcal{N}(E)$ has a binomial distribution:

$$\text{PDF}(\mathcal{N}(E)) = \binom{\ln M}{\mathcal{N}(E)} P(E)^{\mathcal{N}(E)} (1 - P(E))^{\ln M - \mathcal{N}(E)} \tag{2.12}$$

The (mean) number of configuration with energy E is $\overline{\mathcal{N}(E)} = P(E)M$. Therefore

$$\overline{\mathcal{N}(E)} \sim M^{1 - \frac{E^2}{4 \ln M}} (4\pi \ln M)^{-\frac{1}{2}} \gg 1, \quad \text{for} \quad \left|\frac{E}{\ln M}\right| \in (-2, 2) \tag{2.13}$$

$$\overline{\mathcal{N}(E)} << 1, \quad \text{for} \quad \left|\frac{E}{\ln M}\right| > 2. \tag{2.14}$$

This means that, for in the regime $\left|\frac{E}{\ln M}\right| \in (-2, 2)$ there is an exponentially large density of levels and the fluctuations of this density are very small. Thus we have $\overline{\mathcal{N}(E)^n} \sim \overline{\mathcal{N}(E)}^n$. In this regime of energies, the entropy can be estimated by

$$\frac{S(E)}{\ln M} \to \frac{\ln \overline{\mathcal{N}(E)}}{\ln M} = 1 - \frac{1}{4}\left[\frac{E}{\ln M}\right]^2, \ \frac{E}{\ln M} \in (-2, 2), \tag{2.15}$$

On the other hand, for $\left|\frac{E}{\ln M}\right| > 2$ for a generic sample there is no configuration at energy E, $\overline{\mathcal{N}(E)^n} \sim \overline{\mathcal{N}(E)}$.

Using standard thermodynamics formulas, we calculate the inverse temperature

$$\beta = \frac{\partial S}{\partial E} = -E/(2 \ln M) \in (-1, 1) \tag{2.16}$$

and the free energy

$$\mathcal{F} = (E - \beta^{-1} S) \to -\left(\beta + \beta^{-1}\right) \ln M\,, \ |\beta| < 1\,. \tag{2.17}$$

Remark that as $\beta \to 1$, $E/\ln M \to -2$, $S/\ln M \to 0$: the entropy becomes sub-extensive at a non–zero temperature. This is a key signature of disordered systems: it is called the *entropy crisis*, and is responsible for their glassy behaviour and slow dynamics. What happens at lower temperatures? Since the entropy cannot further decrease and cannot increase either, the only possibility is that $S = 0$, and the free energy becomes temperature independent:

$$\mathcal{F} \to -2 \ln M \, , \, \beta \geq 1 \, . \tag{2.18}$$

Equations (2.17) and (2.18) imply a second–order transition at $\beta = \beta_c = 1$, called the *freezing* transition.

The first dominant terms of the free energy for the REM are:

$$\mathcal{F} \to \begin{cases} -(\beta + \beta^{-1}) \ln M + f \, , & \beta < 1 \, , \\ -2 \ln M - \frac{1}{2} \ln \ln M + f \, , & \beta \geq 1 \, . \end{cases} \tag{2.19}$$

The sub-leading term can be computed with more effort (see notes below). Comparing with (2.6) with (2.19) one can note that the two model share the same leading behavior but different subleading ones. The different pre-factors (3/2 vd 1/2) is due to the correlation in the disorders. We wil show that the prefactor 3/2 will also appear from LFT.

2.6 Binding transition

We introduce another transition that will play a role when setting the LFT-log-REM connection. Consider the log-REM model defined in (2.4) for $\alpha = 1$. We add a *deterministic* part of the potential, $V_j \to V_j + U_j$, which has a *logarithmic singularity* at $j = 0$, $U_j = 2\alpha \ln |j|$, such that $\overline{V_j} \to 2\alpha \ln j$. On the other hand, its divergence at $z = 1$ is regularized by $\overline{V_1} = -2\alpha \ln M + O(1)$. The binding transition happens when α is large enough that the thermal particle is trapped at $j = 0$. The easiest way to establish the phase diagram (in the plane of (β, α)) is the following argument (already present in [9], Appendix D, see also [11]). The free-energy of the particle:

$$\text{sitting at } j = 0 \quad F_1 = V_1 \sim -2\alpha \ln M \tag{2.20}$$

$$\text{staying away from } j = 0 \quad F_0 = V_1 \sim -(\beta + \beta^{-1}) \ln M \tag{2.21}$$

$$\tag{2.22}$$

Then, the criterion of

$$\text{No-binding if:} \quad F_0 << F_1, \tag{2.23}$$

which gives

$$\alpha < Q/2 \, , \, Q = \begin{cases} \beta^{-1} + \beta \, , & \beta < 1 \, , \\ 2 \, , & \beta \geq 1 \, . \end{cases} \tag{2.24}$$

The phase diagram is drawn in Figure 4 (Left panel).

In the d-dimensional Euclidean space:

$$\overline{V_j} = U(\mathbf{x}_j) \, , \, U(\mathbf{x}) \sim 2d\alpha \ln |\mathbf{x} - \mathbf{x_1}| \, , \tag{2.25}$$

where $(\mathbf{x_j})_{j=1}^M$ is the lattice of the log-REM. Equation (2.24) gives the condition that the thermal particle is not bound near $\mathbf{x_1}$.

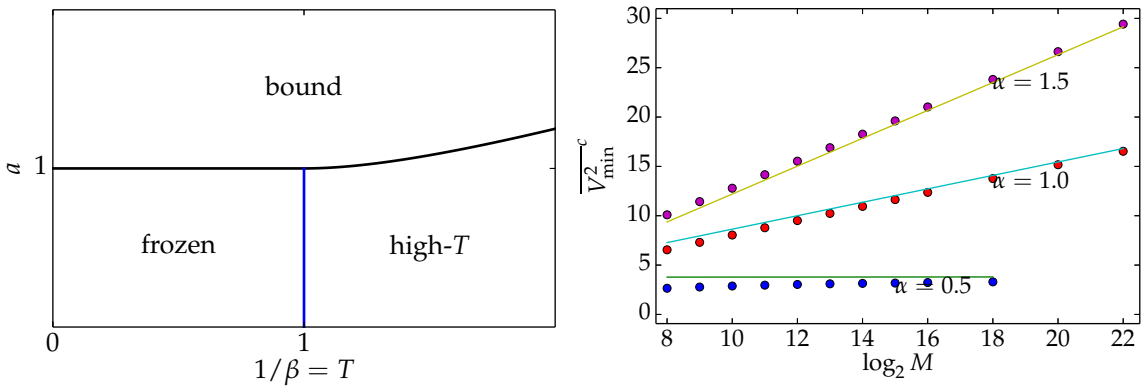

Figure 4. (Left) The phase diagram of log-REM with a logarithmic potential, such as the Morris circular model. The blue vertical line is the freezing transition, while the other (near horizontal) curve is the binding transition line, $a = Q/2$, see eq. (2.24). (Right) The minimum variance of the circular model as a function of the log of system size, compared to $2\ln M + c$ ($\alpha = 1.5$, bound phase), $\ln M + c'$ ($\alpha = 1$, zero temperature critical) and c'' ($\alpha = .5$, frozen phase).

3 Free-energy fluctuations and freezing-duality conjecture

3.1 Laplace transform of the partition function distribution

A central quantity in disordered statistical physics is the Laplace transform of the partition function distribution:

$$G_\beta(x) = \overline{\exp\left(-e^{\beta x}\mathcal{Z}\right)}\,, \tag{3.1}$$

which can be built from the moments of the partition function distribution:

$$G_\beta(x) = \sum_{n=0}^{\infty} \frac{-e^{\beta n x}}{n!}\overline{\mathcal{Z}^n}\,, \tag{3.2}$$

of the *replicated partition sums* $\overline{\mathcal{Z}^n}$, $n = 0, 1, 2, \ldots$. they are the object that is calculated in the replica approach. However, the series, as a function of μ, has usually zero convergence radius around $\mu = 0$, so eq. (3.2) is only useful for formal manipulations, for example. In general the knowledge of the moments $\overline{\mathcal{Z}^n}$ does not completely determines the distribution of $\mathcal{Z}$ (see Carleman theorem)

Using the residue theorem, we can also express the function $G_\beta(x)$ as a contour integral:

$$\int_{r+\mathbf{i}\mathbb{R}} \frac{\mathrm{d}t}{2\pi\mathbf{i}} e^{-tx}\,\beta^{-1}\Gamma(t/\beta)\,\overline{\exp(t\mathcal{F})} = G_\beta(x)\,, \tag{3.3}$$

where r can be chosen such that the vertical contour $r+\mathbf{i}\mathbb{R}$ is at the right of all the poles of the integrand. The above expression can be used as a non–rigorous re–summation of the series eq. (3.2), *if* we can continue $\overline{\mathcal{Z}^n}$ to *complex* n. Another useful relation is obtained by inverting the above Laplace transform:

$$\overline{\exp(t\mathcal{F})} = \int_0^\infty d\mathcal{F} e^{t\mathcal{F}} P(\mathcal{F}) = \int_0^\infty e^{tx} G_\beta(x) dx = \frac{1}{\Gamma(t/\beta)} \int_0^\infty dx\; e^{tx} G_\beta(x) = \tag{3.4}$$

$$= \frac{1}{\Gamma(1+t/\beta)} \int_0^\infty dx\; e^{tx}(-\partial_x G_\beta(x)) \tag{3.5}$$

Note that at $\beta \to \infty$, the $P(\mathcal{F}) = -\partial_x G_\infty(\mathcal{F})$. So the function $G_\beta(\mathcal{F})$ determines the behavior of the minima of these random set.

Finally, it is convenient to introduce a random variable g which has the standard Gumbel distribution $P(g) = \exp(g + e^{-g})$. Using the property:

$$\overline{\theta(x-g)} = \int_x^\infty dg P(g) = \exp(-e^{-x}), \quad \overline{e^{tg}} = \Gamma(1-t) \tag{3.6}$$

where $\theta(x)$ is the Heaviside function, the $G_\beta(x)$ can be seen as a cumulative distribution function. Indeed, eq. (3.1) implies

$$G_\beta(x) = \overline{\exp\left(-e^{\beta(x-\mathcal{F})}\right)} = \overline{\theta(-\beta(x-\mathcal{F})-g)} = \overline{\theta([\mathcal{F}-g/\beta]-x)}, \tag{3.7}$$

where with the notation $\overline{A(g,\mathcal{Z})}$ stands for the average over the disorder (in $\mathcal{Z}$) and over g.

3.2 REM: Correction terms and the Gumbel law of the fluctuation

Here, we give an elegant replica-free method (provided in [12], last appendix) to calculate the distribution of $\mathcal{F}$ at any temperature.

For the REM (see [12], last appendix), for which V_j's are independent:

$$G_\beta(x) = [\gamma_\beta(x)]^M \overset{M\to\infty}{\longrightarrow} e^{\hat{\gamma}_\beta(y)}, \ \hat{\gamma}_\beta = \lim_{M\to\infty}\left(M(\gamma_\beta - 1)\right), \tag{3.8}$$

$$\gamma_\beta(x) = \int_{\mathbb{R}} \frac{\mathrm{d}v e^{-\frac{v^2}{4\ln M}}}{\sqrt{4\pi \ln M}} \exp(-e^{\beta(x-v)}). \tag{3.9}$$

The last quantity can be calculated by a Hubbard-Stratonovich transform: *i.e.*, we insert into the above equation the identity

$$\frac{e^{-\frac{v^2}{4\ln M}}}{\sqrt{4\pi\ln M}} = \int_{\mathbb{R}-\mathbf{i}\epsilon} \frac{\mathrm{d}p}{2\pi} e^{-pv+p^2\ln M}, \ \epsilon > 0, \tag{3.10}$$

and then integrate over v in terms of the Gamma function,

$$\gamma_\beta(x) = \int_{\epsilon+\mathbf{i}\mathbb{R}} \frac{\mathrm{d}p}{2\pi\mathbf{i}} e^{p^2\ln M - xp} \int_{\mathbb{R}} \mathrm{d}v e^{-p(v-x)} \exp\left(-e^{\beta(x-v)}\right) \tag{3.11}$$

$$= \int_{\epsilon+\mathbf{i}\mathbb{R}} \frac{\mathrm{d}p}{2\pi\mathbf{i}} e^{p^2\ln M - xp} \beta^{-1}\Gamma(p/\beta) \tag{3.12}$$

$$= 1 + \int_{-\epsilon+\mathbf{i}\mathbb{R}} \frac{\mathrm{d}p}{2\pi\mathbf{i}} e^{p^2\ln M - xp}\Gamma(p/\beta) \tag{3.13}$$

In eq. (3.10), the contour is at the right of the imaginary axis so that the v-integral in eq. (3.11) converges at $v \to +\infty$. In eq. (3.13) we move the contour across the imaginary axis, picking up the residue of the Gamma pole at $p = 0$, which gives 1 by the Cauchy's formula.

The remaining integral shall be analysed by the saddle point/steepest descent method, the saddle point of (3.13) being at $p_* = x/(2\ln M)$. For this, (3.8) implies that one should consider the regime of y where $\hat{\gamma}_\beta \sim O(1)$, or $\gamma_\beta \sim 1/M$. Expectedly, such regimes are in agreement with eq. (2.17) and (2.18). So the analysis is different in the two phases (see Figure 5 for an illustration):

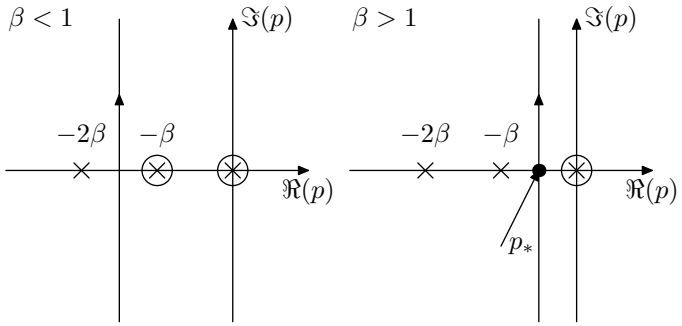

Figure 5. Illustrations of the deformed contour integral. The Gamma poles at indicated with a cross. The residue of the pole at 0 gives the term 1 in eq. (3.13). *Left*: In the $\beta < 1$ phase, the dominant contribution comes from the pole at $-\beta$. *Right*: In the $\beta > 1$ phase, the dominant contribution comes from the saddle point at $p_* > -\beta$.

1. $\beta < 1$. Eq. (2.17) implies the relevant regime should be $x = -(\beta + \beta^{-1}) \ln M + y$, $y \sim o(\ln M)$. But then $p_*/\beta < -1$, so to deform the contour to cross the saddle point, one has to pick up residues of some Gamma poles. It is not hard to check that the pole at $p = -\beta$ has dominant contribution:

$$\hat{\gamma}_\beta(x) = -e^{\beta y} \overset{(3.8)}{\Rightarrow} G_\beta(y) \overset{M\to\infty}{=} \exp\left(-e^{\beta y}\right) , \; x = y - (\beta + \beta^{-1}) \ln M \, . \tag{3.14}$$

   By eq. (**??**), this means that

$$\overline{\theta(\mathcal{F} - g/\beta - x)} = \exp(-\exp(\beta(x + (\beta + \beta^{-1}) \ln M))) \, ,$$

   i.e., the PDF of $\mathcal{F} - g/\beta$ is equal to that of $-g/\beta - (\beta + \beta^{-1}) \ln M$ (where we recall that g is a standard Gumbel random variable independent of $\mathcal{F}$). As a consequence, the free energy becomes deterministic in the thermodynamic limit:

$$\mathcal{F} \equiv -(\beta + \beta^{-1}) \ln M \, . \tag{3.15}$$

2. $\beta > 1$. Eq. (2.18) points to the regime $x = -2 \ln M + o(\ln M)$, so $p_*/\beta > -1$, thus no pole-crossing is needed to deform the contour to the saddle point. Yet, $x = -2 \ln M$ would give $\gamma_\beta = 1 + M^{-1}(4\pi \ln M)^{-\frac{1}{2}}$, with an extra correction from the Jacobian; so the correct regime of x should be $\sim -2 \ln M + \frac{1}{2} \ln \ln M$. More precisely, one can check the following:

$$G_\beta(x) \overset{M\to\infty}{\longrightarrow} \exp\left(-e^{y}\right) , \; x = y - 2 \ln M + \frac{1}{2} \ln \ln M + c_\beta \, , \tag{3.16}$$

   where $c_\beta = \frac{1}{2} \ln(4\pi) - \ln \Gamma(1 - \beta^{-1})$. It diverges at $\beta \to 1_+$, ensuring the matching with the $\beta < 1$ phase.

   In terms of eq. (**??**), the equation (3.16) means that the PDF of the convolution $(\mathcal{F} - g/\beta)$ is *temperature independent* in the $\beta > 1$ phase, up to a translation. This is a remarkable fact that further justifies calling the $\beta = 1$ transition *freezing*: not only the extensive free energy freezes, but also its fluctuation, *after convolution with* g/β. It should be stressed that the free energy distribution does not freeze, because it is obtained from that of $\mathcal{F} - g/\beta$ by undoing the convolution with $-g/\beta$

3.3 Replica approach and analytic computation: the circular model example

A common way to construct a 1d log-REM them is to restrict the 2D Gaussian free field to some 1D curve, such as the unit circle or the interval $[0, 1]$. It turns out that, in these two geometries, the limit distribution $g(y)$ can be exactly calculated. For this, let us write down the (continuous, formal) partition function of the circular model:

$$Z = \int_0^{2\pi} \frac{\mathrm{d}\theta}{2\pi} \exp\left(-\beta\phi(e^{\mathrm{i}\theta})\right) \, , \overline{\phi(z)\phi(w)} = -2\ln(|z-w|) \, , \, \overline{\phi(z)} = 0 \, . \tag{3.17}$$

Then, we proceed by the *replica trick*, which starts by calculating integer moments of Z:

$$\overline{Z^n} = \int_0^{2\pi} \prod_{a=1}^{n} \frac{\mathrm{d}\theta_a}{2\pi} \overline{\exp\left(-\beta \sum_{a=1}^{n} \phi(z_a)\right)} \, , \; z_a = e^{\mathrm{i}\theta_a} \, . \tag{3.18}$$

To compute this, we use the Wick theorem, which holds any Gaussian variable V

$$\overline{\exp(V)} = \exp\left(\overline{V} + \frac{1}{2}\overline{V^2}^c\right) \, , \; \overline{V^2}^c = \overline{V^2} - \left(\overline{V}\right)^2 \tag{3.19}$$

applied to $V = -\beta \sum_{a=1}^{n} \phi(z_a)$:

$$\begin{aligned} \overline{\exp(V)} &= \exp\left(\frac{1}{2}\sum_{a=1}^{n} \beta^2 \overline{\phi(z_a)^2} + \beta^2 \sum_{a<a'} \overline{\phi(z_a)\phi(z_{a'})}\right) \\ &= \prod_{a=1}^{n} e^{\frac{1}{2}\beta^2 \overline{\phi(z_a)^2}} \prod_{1\le a<b\le n} |z_a - z_b|^{-2\beta^2} \, . \end{aligned}$$

In the second equation we applied (3.17). Plugging into eq. (3.18), we have

$$\overline{Z^n} = \int_0^{2\pi} \prod_{a=1}^{n} \frac{\mathrm{d}\theta_a}{2\pi} \prod_{a=1}^{n} e^{\frac{1}{2}\beta^2 \overline{\phi(z_a)^2}} \prod_{1\le a<b\le n} |z_a - z_b|^{-2\beta^2} \, , \tag{3.20}$$

As the regularized value of $\overline{\phi(z)^2}$ is independent of z, the term involving it in (3.20) can be absorbed into a normalization of Z, which is equivalent to a shift in the free energy, immaterial to the calculation of its limit distribution. So, we can set $\overline{\phi(z)^2} = 0$. Now, eq. (3.20), with $\overline{\phi^2(z)} = 0$, is known as the Dyson integral [13]

$$\overline{Z^n} = \int_0^{2\pi} \prod_{a=1}^{n} \frac{\mathrm{d}\theta_a}{2\pi} \prod_{1\le a<b\le n} |z_a - z_b|^{-2\beta^2} = \frac{\Gamma(1-n\beta^2)}{\Gamma(1-\beta^2)^n} \, , \tag{3.21}$$

We will use the freedom to normalize the partition function by looking at the quantity:

$$Z_e = \Gamma(1-\beta^2) Z \tag{3.22}$$

The key *non-rigorous* step of the replica trick is to analytically continue eq. (3.21) to generic value of $n \in \mathbb{C}$.

$$\overline{\exp(tF)} = \overline{Z_e^{-t/\beta}} = \Gamma(1+t\beta) \, . \tag{3.23a}$$

From the (3.3):

$$g_\beta(y) = \int_{\mathbf{i}\mathbb{R}+\epsilon} \frac{\mathrm{d}t}{2\pi\mathbf{i}t}\, e^{-ty}\, \Gamma(1+t\beta)\Gamma(1+t/\beta)\,. \tag{3.23b}$$

Now, the key point is that equations (3.23) hold only in the phase $\beta < 1$. The basic reason behind this is that the naive continuum formalism presented just now is invalid in the $\beta > 1$ phase where the metastable states, and therefore the physics at the lattice scale, have to be taken into account (producing the 1 step replica symmetry breaking).

3.3.1 Freezing–duality conjecture

In log-REM, dual quantities in the $\beta < 1$ phase freeze in the $\beta > 1$ phase.

In this case we have

$$g(y)|_{\beta>1} = g(y)|_{\beta=1} = \int_{\mathbf{i}\mathbb{R}+\epsilon} \frac{\mathrm{d}t}{2\pi\mathbf{i}t}\Gamma(1+t)^2 e^{-ty} = 2e^{y/2}K_1(2e^{y/2})\,, \tag{3.24}$$

K_n denoting the Bessel K-function. In particular, since the pole at $t = -1$ is a double one, we have the left tail $g(y) \sim A\,|y|\,e^y, y \to -\infty$, verifying the freezing scenario prediction.

To this day, this conjecture is verified in all exact solvable log-REM, but the reason behind has not been understood. The duality observed in log-REM echoes those in β–random matrix theory [14] (which has been applied to study log-REM, see [15, 16]) and in 2D conformal field theory [17, 18]. The latter is not merely a superficial reminiscence: as we shall see in section 5, log-REM are closely related to the LFT.

4 Gibbs measure and multi-fractality of logREMs

We review some useful observables to better characterize the high temperature and low-temperature phases. The central quantity is the normalized *Gibbs measure*:

$$p_{\beta,j} = \frac{1}{\mathcal{Z}} e^{-\beta V_j}\,,\ j = 1, \ldots, M\,,\ . \tag{4.1}$$

4.1 Overlap distribution

4.1.1 Definition of the overlap q

The notion of overlap in disordered system is clearly understood in the example of the Directed Polymer on the Cayley Tree, DPCT, (which is another important version of log-REM models) A It is defined on a Cayley tree (see Figure 6 for an illustration), described by its branching number κ and the number of generations $n \in \mathbb{N}$, so that the total number of leaves is $M = \kappa^n$. To each edge, we associate an independent energy, which is a centred Gaussian variable of variance $2\ln\kappa$. Directed polymer (DP) are by definition the simple path from the tree root to one of the leaves, and its energy $V_i, i = 1, \ldots, M$ is the sum of those of its edges. Therefore, the energy of each individual DP is a centred Gaussian with variance $n \times 2\ln\kappa = 2\ln M$, identical to the REM, moreover, the correlation of any two DP's is

$$\overline{V_i V_j} = 2\hat{\mathsf{q}}_{ij} \ln\kappa\,, \tag{4.2}$$

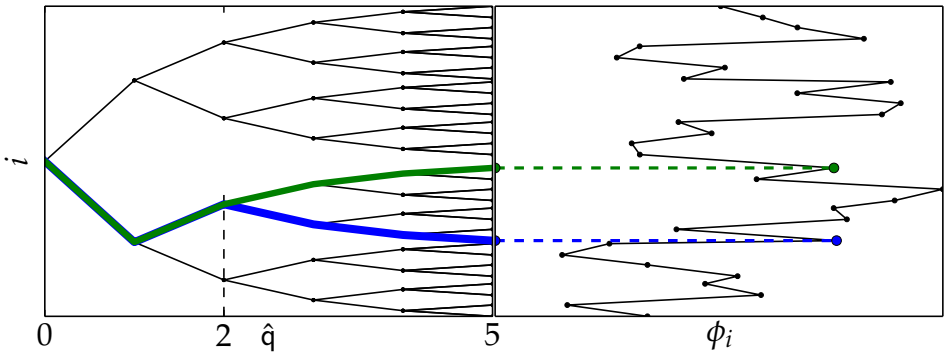

Figure 6. A Cayley tree of branching number $\kappa = 2$ and $n = 5$. Two directed polymers are drawn in bold and different colours. They have common length $\hat{\mathsf{q}} = 2$, and overlap $\mathsf{q} = .4$. On the right panel, a sample of the energies of the directed polymers is plotted.

where $\hat{q}_{ij}$ is the common length of the DP's i and j. For example, the matrix for $\kappa = 2$ and $n = 2$ is

$$(\hat{\mathsf{q}}_{ij}) = \begin{pmatrix} 2 & 1 & 0 & 0 \\ 1 & 2 & 0 & 0 \\ 0 & 0 & 2 & 1 \\ 0 & 0 & 1 & 2 \end{pmatrix} . \tag{4.3}$$

A closely related quantity is the *overlap*, defined by a simple rescaling:

$$\mathsf{q}_{ij} \overset{\text{def.}}{=} \frac{\overline{V_i V_j}}{2 \ln M} = \frac{\hat{\mathsf{q}}_{ij}}{n} \in [0, 1] . \tag{4.4}$$

The overlap is an important notion of the spin glass theory: its definition depends on the model, so as to measure the "similarity" of two configurations

The overlap in Euclidean log-REM has the same definition as hierarchical ones:

$$\mathsf{q}_{jk} = \frac{\overline{V_j V_k}^c}{2 \ln M} \tag{4.5}$$

4.1.2 Overlap distribution: $M \to \infty$ limit

The overlap distribution $P(\mathsf{q})$ of two independent thermal particles in one random potential is :

$$P(\mathsf{q}) \overset{\text{def.}}{=} \overline{\sum_{j,k} p_{\beta,j} p_{\beta,k} \delta(\mathsf{q}_{jk} - \mathsf{q})} \tag{4.6}$$

($P(\mathsf{q})$ turns out to be directly related to the replica symmetry breaking parameter $m(\mathsf{q})$).

In the $M \to \infty$ limit, one has: overlap distribution obeys the "zero–one" law:

$$P(\mathsf{q}) = \begin{cases} \delta(\mathsf{q}) , & \beta < 1 , \\ \beta^{-1} \delta(\mathsf{q}) + (1 - \beta^{-1}) \delta(1 - \mathsf{q}) , & \beta \geq 1 . \end{cases} \tag{4.7}$$

Recalling the relation between the overlap and the (Euclidean) distance (eq. (**??**)), this means that two thermal particles in a log–correlated potential are either of system size

scale ($\mathsf{q}=0$), or of lattice spacing scale ($\mathsf{q}=1$); the $\beta>1$ phase is characterized by the non-vanishing probability of the latter case.

A simple illustration of the above picture can be provided by the positions of deepest minima in a log-correlated potential, see Figure 2.2 for a 1D example. We can see that they form clusters of lattice spacing size, while different clusters are separated by a system-scale distance. It is intuitive but not easy to show that the overlap is related with minima positions;

We will use the Liouville field theory to predict some finite M corrections of the above formulas. Our final result will be given in (5.52)

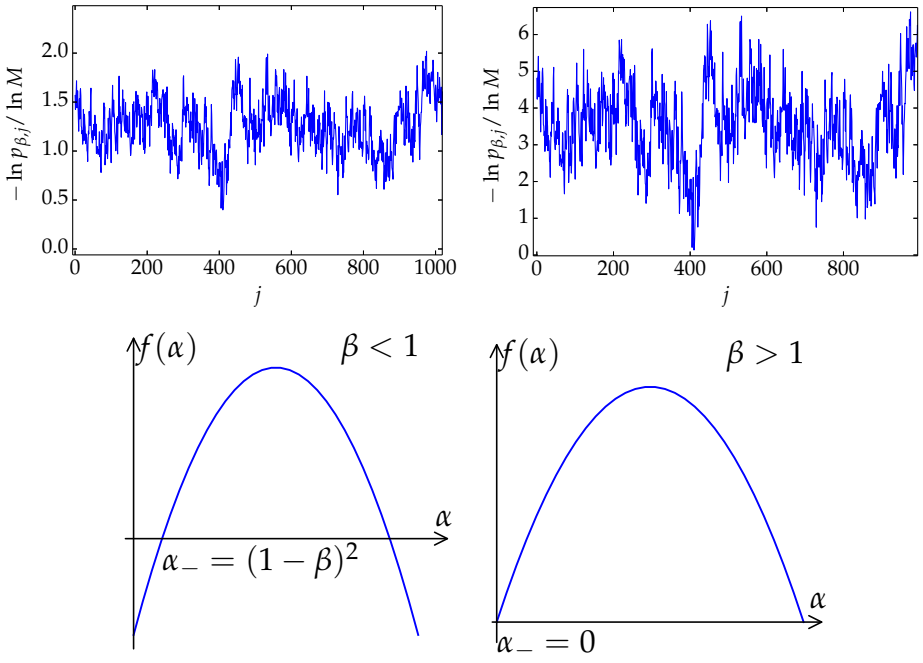

Figure 7. Left: The log-scale colour plot of the Gibbs measure of a log-REM of 2DGFF on a torus.

4.2 Multifractal spectrum: $f(\alpha)$

As we can see in figure 7, $p_{\beta,j}$'s magnitude spans a large range. The *multi–fractal spectrum* of $p_{\beta,j}$ is defined by making a histogram of $-\frac{\ln p_{\beta,j}}{\ln M}$, and then "plot" it the log scale:

$$f(\alpha)=\frac{1}{\ln M\mathrm{d}\alpha}\ln\left|\left\{j:-\frac{\ln p_{\beta,j}}{\ln M}\in[\alpha,\alpha+\mathrm{d}\alpha]\right\}\right|,\alpha\geq 0 \tag{4.8a}$$

$$\Leftrightarrow\left|\left\{j:p_{\beta,j}\sim M^{-\alpha}\right\}\right|=M^{f(\alpha)}\times\text{corrections}, \tag{4.8b}$$

where $|X|$ denotes the number of elements in the set X. In the above equations, $f(\alpha)$ is defined for any sample of disorder (V_j). However, as $M\to\infty$, $f(\alpha)$ is expected to become deterministic, and is called the multi–fractal spectrum. Note that the definitions eq. (4.8) applies to any long sequence of positive numbers $p_j, j=1,\dots,M$.

For the REM and log-REM, $f(\alpha)$ is quadratic [19]:

$$f(\alpha)=\frac{4(\alpha_+-\alpha)(\alpha-\alpha_-)}{(\alpha_+-\alpha_-)^2},\alpha_-=\begin{cases}(1-\beta)^2 & \beta<1,\\ 0 & \beta\geq 1,\end{cases}\quad \alpha_+=\alpha_-+4\beta, \tag{4.9}$$

see figure 7 for plots in the two phases. Note that the freezing transition manifests itself also in the non-analytic β-dependence of $f(\alpha)$ at $\beta = 1$.

A simple derivation of eq. (4.9) goes as follows. By eq. (4.1), $\alpha_j = \beta(V_j - \ln \mathcal{F})/\ln M$. Now since $\mathcal{F}/\ln M$ is deterministic as given by eq. (2.6), and V_j is a centred Gaussian of variance $2\ln M$. So when $M \to \infty$, α_j is a Gaussian of mean $\beta^2 + 1$ and variance $2\beta^2/\ln M$. Therefore, the normalized probability distribution of α is

$$\ln \mathrm{P}(\alpha) = \begin{cases} -\frac{(\alpha-\beta^2-1)^2}{4\beta^2} + o(\ln M)\,, \\ -\frac{(\alpha-2\beta)^2}{4\beta^2} + o(\ln M)\,. \end{cases} \tag{4.10}$$

Plugging this into $f(\alpha) = \frac{1}{\ln M} \ln (M\mathrm{P}(\alpha))$ gives eq. (4.9) after some algebra. The tacit assumption behind the above reasoning is that the correlation between (V_j) and $\mathcal{F}$ has no effect on $f(\alpha)$. Indeed, as we will see later (section 5.4.3), the effect of the correlations are limited to the sub–leading order.

4.3 Inverse Partition Ratio

The (generalized) IPR are important observables closely related to the multi–fractal spectrum. The IPR are defined in terms of its Gibbs measure $p_{\beta,j}, j = 1, \ldots, M$, as follows:

$$P_q = \sum_{j=1}^{M} p_{\beta,j}^q\,,\ q \geq 0\,. \tag{4.11}$$

IPR for $q < 0$ are seldom considered. This definition is as general as the multi–fractal spectrum: in particular, it can be calculated for each disorder realization. In the large system $M \to \infty$ limit, we can compute its leading behaviour using the definition of the multi–fractal spectrum eq. (4.8), and the saddle point approximation

$$P_q = \int_I \mathrm{d}\alpha\, M^{-q\alpha + f(\alpha)} = M^{-\tau_q} \times \text{corrections}\,, \tag{4.12}$$

$$\text{where } \tau_q = \min_{\alpha \in I} \left[q\alpha - f(\alpha)\right]\,. \tag{4.13}$$

Here, τ_q is called the multi–fractal *exponent*. As a function of q, it is calculated as the Legendre transform of the multi–fractal spectrum $f(\alpha)$, eq. (4.13). In general, it is calculated by solving the equation $\partial_\alpha f(\alpha_q) = q$ for α_q. The solution is unique if since $f(\alpha)$ is convex. This is the case for log-REM, see eq. (4.9), and we have

$$\alpha_q = \begin{cases} -2q\beta^2 + \beta^2 + 1\,, & \beta \leq 1 \\ -2q\beta^2 + 2 & \beta > 1\,. \end{cases} \tag{4.14}$$

In general, α_q has the following interpretation: the dominating contribution to P_q comes from those points $p_{\beta,j} \sim M^{-\alpha_q}$. When q increases, α_q decreases. In terms of α_q, the multi–fractal exponent is given as $\tau_q = q\alpha_q - f(\alpha_q)$. After simple algebra, one finds for the log-REM:

$$\tau_q = q\beta\,(Q - q\beta) - 1\,,\ Q = \begin{cases} \beta + \beta^{-1} & \beta \leq 1\,, \\ 2 & \beta > 1\,. \end{cases} \tag{4.15}$$

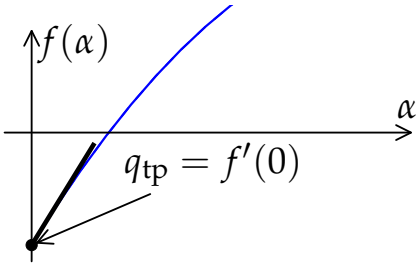

Figure 8. Illustration of the termination point transition in the annealed ensemble, see eq. (4.16). The multi–fractal spectrum is defined until $\alpha = 0$.

The above notation is suggested by the LFT, see section 5.

The *annealed* ensemble (Figure 8) concerns the *mean value* $\overline{P_q}$, averaged over *all* disorder samples. So, even if $f(\alpha) < 0$, Gibbs measure values $p_{\beta,j} \sim M^{-\alpha}$ will be present in some rare samples, and the above transition is absent: eq. (4.15) is true beyond $q = \beta^{-1}$. However, since $p_{\beta,j} \leq 1$ by normalization, so α can never be negative. Therefore, when $q > q_{tp} = f'(0) = Q/(2\beta)$ (in the two phases, with Q defined in eq. (**??**)), the value α_q given by eq. (4.14) is non-physical and should be replaced by $\alpha_q^{\rm ann.} = 0$. So the annealed ensemble exponents are

$$\tau_q^{\rm ann.} = \begin{cases} q\beta\,(Q - q\beta) - 1\,, & q < Q/(2\beta)\,, \\ Q^2/4 - 1\,, & q \geq Q/(2\beta)\,. \end{cases} \tag{4.16}$$

The non-analyticity of $\tau_q^{\rm ann.}$ has also different names: We will use the term *termination point transition* in this work.

The above discussion is limited to the leading behaviours (exponents).

We will explore the sub–leading corrections: in particular, in the annealed ensemble, they will be predicted for the first time using LFT.

5 Liouville field theory (LFT) and log-REM

5.1 The LFT and 2D GFF

We will use the LFT functional integral representation. This is defined, on any closed surface Σ, from the action $\mathcal{S}_b$:

$$\mathcal{S}_b = \int_\Sigma \left[\frac{1}{16\pi} (\nabla\varphi)^2 - \frac{1}{8\pi} Q\hat{R}\varphi + \mu e^{-b\varphi} \right] \mathrm{d}A\,, \tag{5.1}$$

where μ is the coupling constant, $\hat{R}$ is the Ricci curvature and $\mathrm{d}A$ the surface element [1]. In our case, we will then consider the surface $\Sigma = \mathbb{C} \cup \{\infty\}$ has the topology of a sphere with the curvature concentrated at ∞ and vanishing elsewhere: $\hat{R}(z) = 8\pi\delta^2(z - \infty)$.

[1] For instance for the unit sphere:

$$\mathrm{d}A = \frac{2}{(1 + |z|^2)^2} \mathrm{d}^2 z\,,\ \mathrm{d}^2 \overset{\text{def.}}{=} \mathrm{d}x \wedge \mathrm{d}y\,, \tag{5.2}$$

Here, φ is the Liouville field, $\mu > 0$ is the coupling constant (also called the "cosmological constant"), $b > 0$ is the parameter defining the LFT, and

$$Q = b + b^{-1} \,. \tag{5.3}$$

This coefficient of the coupling of the Liouville field to the curvature is the most important ingredient of LFT, and guarantees its conformal invariance among other properties, see [20] for detailed demonstration. We recall (see Sylvain Ribault lectures) that the *central charge* of LFT is

$$c = 1 + 6Q^2 \geq 25 \,, \quad \text{if } b \in \mathbb{R} \,, \tag{5.4}$$

The ones considered in LFT are those of *vertex operators*, defined as exponential fields

$$\mathcal{V}_a(w) = e^{-a\varphi(w)} \,, \tag{5.5}$$

where a is called the *charge* of the vertex operator. The n-point correlation functions are defined by the usual functional integral

$$\left\langle \prod_{i=1}^{n} \mathcal{V}_{a_i}(w_i) \right\rangle_b = \int \mathcal{D}\varphi \, e^{-\mathcal{S}_b} \prod_{i=1}^{n} e^{-a_i \varphi(w_i)} \,. \tag{5.6}$$

5.1.1 Integration of zero–mode

The connection between eq. (5.6) and 2D GFF was established by Goulian and Li [21] and is the basis of the recent rigorous developments [22].

The starting point is the decomposition of the Liouville field into a *zero–mode* φ_0 and a fluctuating part $\tilde{\varphi}$, and a similar factorization of the functional integral:

$$\varphi = \varphi_0 + \tilde{\varphi} \,, \text{ such that } \int_\Sigma \tilde{\varphi} \mathrm{d}A = 0 \,, \; \int \mathcal{D}\varphi = \int_{\mathbb{R}} \mathrm{d}\varphi_0 \times \int \mathcal{D}\tilde{\varphi} \,. \tag{5.7}$$

The action eq. (5.1) can be then written as

$$\begin{aligned} \mathcal{S}_b &= \int_\Sigma \left[\frac{1}{16\pi} (\nabla\tilde{\varphi})^2 - \frac{1}{8\pi} Q \hat{R} \tilde{\varphi} \right] \mathrm{d}A + \mu e^{-b\varphi_0} \int_\Sigma e^{-b\tilde{\varphi}} \mathrm{d}A + \varphi_0 \int_\Sigma \frac{1}{8\pi} Q \mathrm{d}A \\ &= \int_\Sigma \left[\frac{1}{16\pi} (\nabla\tilde{\varphi})^2 - \frac{1}{8\pi} Q \hat{R} \tilde{\varphi} \right] \mathrm{d}A + \mu e^{-b\varphi_0} Z_0 + \varphi_0 Q \chi / 2 \,, \end{aligned} \tag{5.8}$$

where in the second line we defined the continuum partition function

$$Z_0 \overset{\text{def.}}{=} \int_\Sigma e^{-b\tilde{\varphi}} \mathrm{d}A \,, \tag{5.9}$$

and used the Gauss-Bonnet theorem

$$\int_\Sigma \hat{R} \mathrm{d}A = 4\pi\chi \,, \tag{5.10}$$

where χ is the *Euler characteristic* of the surface Σ. It depends only on the topology of the surface: for a sphere, $\chi = 2$, for a torus, $\chi = 0$, and $\chi = 2 - 2g$ for general closed surface with genus g handles. We can decompose similarly the vertex operator eq. (5.5)

$\mathcal{V}_a(z) = e^{-a\varphi_0} e^{-a\tilde{\varphi}}$. Plugging this and eq. (5.8) and into eq. (5.6), we can integrate out the dependences on the zero mode:

$$\left\langle \prod_{i=1}^{n} \mathcal{V}_{a_i}(w_i) \right\rangle_b = \int \mathcal{D}\tilde{\varphi}\, e^{-\int_\Sigma \left[\frac{1}{16\pi}(\nabla\tilde{\varphi})^2 - \frac{1}{8\pi} Q\hat{R}\tilde{\varphi}\right] \mathrm{d}A + \sum_{i=1}^n a_i \tilde{\varphi}(w_i)} \times \int_{\mathbb{R}} \mathrm{d}\varphi_0 \exp(-\mu e^{b\varphi_0} Z_0) e^{\left(Q\chi/2 - \sum_{i=1}^n a_i\right)\varphi_0}$$

The zero mode integral (the second line) is convergent if and only if

$$s \overset{\text{def.}}{=} \sum_{i=1}^{n} a_i - Q\chi/2 > 0\,, \tag{5.11}$$

. When eq. (5.11) is satisfied, the φ_0 integral can be evaluated using $\Gamma[z] = \int_0^\infty e^z t^{z-1}$ and the change of variables $\varphi_0 \to y = \mu e^{b\varphi_0}$:

$$\left\langle \prod_{i=1}^{n} \mathcal{V}_{a_i}(w_i) \right\rangle_b = \frac{\Gamma\left[\frac{s}{b}\right]}{b\mu^{\frac{s}{b}}} \int \mathcal{D}\tilde{\varphi}\, e^{-\int_\Sigma \left[\frac{1}{16\pi}(\nabla\tilde{\varphi})^2 - \frac{1}{8\pi} Q\hat{R}\tilde{\varphi}\right] \mathrm{d}A + \sum_{i=1}^n a_i \tilde{\varphi}(w_i)} Z_0^{-s/b} \tag{5.12}$$

We see now that the terms in the exponential become at most quadratic, and can be interpreted in terms of a *free* field. In order to be completely clear, let us denote by ϕ the 2D GFF on Σ. Its Green function is the solution to Poisson equation

$$\overline{\phi(z)\phi(w)} = K(z,w)\,,\ \Delta_z K(z,w) = 8\pi\left(V^{-1} - \delta_{z,w}\right)\,,\ \int_\Sigma K(z,w)\mathrm{d}A = 0\,, \tag{5.13}$$

where $V = \int_\Sigma \mathrm{d}A$ is the total area of the surface and Δ is the Laplace–Beltrami operator on Σ. Since $\tilde{\varphi}$ has no zero mode by eq. (5.7), the functional integral over it is proportional to an average over the 2D GFF defined on the surface Σ:

$$\int \mathcal{D}\tilde{\varphi}\, e^{-\int_\Sigma \left[\frac{1}{16\pi}(\nabla\tilde{\varphi})^2\right]} \mathcal{O}[\tilde{\varphi}] = N_\Sigma \overline{\mathcal{O}[\phi]}\,. \tag{5.14}$$

Here, $\mathcal{O}[\dots]$ denotes any observable, and N_Σ is a normalization factor (the partition function of free boson on Σ), and $\overline{[\dots]}$ in the right hand side denotes the average over ϕ.

From now on, we will identify ϕ and $\tilde{\varphi}$, *e.g.* in (5.9). Combined with (5.12) we have the following representation of LFT correlation functions in terms of 2D GFF:

$$\left\langle \prod_{i=1}^{n} \mathcal{V}_{a_i}(w_i) \right\rangle_b = C\overline{\exp\left(\int_\Sigma Q\hat{R}\phi/2 - \sum_{i=1}^{n} a_i\phi(w_i)\right) Z_0^{-s/b}}\,, \tag{5.15}$$

where $C = \Gamma(s/b) b^{-1} \mu^{-\frac{s}{b}} N_\Sigma$. Note that the dependence on the coupling constant μ is included in this global factor.

We remark that, if we neglected the Seiberg bound requirement, eq. (5.11), and supposed that $-s/b = n$ was an integer in eq. (5.15), its right hand side would be a Coulomb–gas integral over n moving charges on the 2D surface. This is reminiscent of the Coulomb–gas representation of correlation functions in minimal CFT [17], which describes

critical statistical models in 2D, like the Ising model. Now, by observing the constant below eq. (5.15), we see that the residue at $-s/b = n$ of the correlation function in the left–hand side of eq. (5.15) is given by a Coulomb–gas integral; so, a crucial step of the bootstrap solution of LFT can be seen as the *analytical continuation* of the Coulomb gas integrals to non–integer values of n. In the literature, the equation $-s/b = n, n = 1, 2, 3, \ldots$ is also called a "screening condition". We stress that in our applications, this will never be satisfied, because eq. (5.11) will always hold: $s > 0$.

5.2 LFT and 2d log-REM

Consider, on the one hand the LFT correlation function $\left\langle \prod_{j=1}^{\ell} \mathcal{V}_{a_j}(w_j) \prod_{i=1}^{k} \mathcal{V}_{q_i b}(z_i) \right\rangle_b$ with the following constraints on the parameters $a_1, \ldots, a_\ell, q_1 b, \ldots, q_k b$,

$$\sum_{i=1}^{\ell} a_i = Q\chi/2\,,\; b \leq 1\,, \forall a_j < \frac{Q}{2}\,,\; \forall q_i < \frac{Q}{2b}\,. \tag{5.16}$$

On the other hand, let $U(z)$ be a deterministic logarithmic potential defined by the Laplace equation, eq. (5.21) below:

$$\Delta_z U(z) = 8\pi(a_1\delta_{z,w_1} + \cdots + a_\ell \delta_{z,w_\ell}) - Q\hat{R}\,. \tag{5.17}$$

We defined the Gibbs measure $p_b(z)$ (at inverse temperature $\beta = b \leq 1$) of a log-REM made of the 2D GFF plus $U(z)$ (5.28):

$$p_b(z) \overset{\text{def.}}{=} \frac{1}{Z} e^{-b(\phi(z)+U(z))}\,,\; Z \overset{\text{def.}}{=} \int e^{-b(\phi+U)} \mathrm{d}A\,, \tag{5.18}$$

Then, we have the exact correspondence:

$$\left\langle \prod_{j=1}^{\ell} \mathcal{V}_{a_j}(w_j) \prod_{i=1}^{k} \mathcal{V}_{q_i b}(z_i) \right\rangle_b = C' \overline{\prod_{i=1}^{m} p_b^{q_i}(z_i)}\,, \tag{5.19}$$

where C' is a constant independent of (z_i).

5.2.1 Complete–the–square trick

To show the above quoted result, we need to separate the vertex operators into two groups to which we associate different meaning. Let $\ell < n$ and consider the first ℓ vertex operators. For the mapping to be correctly established, we shall require that their sum

$$\sum_{i=1}^{\ell} a_i = Q\chi/2\,, \tag{5.20}$$

where χ is the Euler characteristics. This is indeed the *charge neutrality condition* (which is *not* the screening condition mentioned above) of the following Poisson equation for $U(z)$:

$$\Delta_z U(z) = 8\pi(a_1\delta_{z,w_1} + \cdots + a_\ell \delta_{z,w_\ell}) - Q\hat{R}\,, \tag{5.21}$$

where the Dirac deltas are respect to the surface integral $\int \mathrm{d}A$. The necessary and sufficient condition for eq. (5.21) to have a solution is that the integral right hand side over

the surface vanishes. But this is precisely guaranteed by eq. (5.20) and the Gauss-Bonnet theorem eq. (5.10):

$$\int \mathrm{d}A \left[8\pi(a_1\delta_{z,w_1} + \cdots + a_\ell \delta_{z,w_\ell}) - Q\hat{R}\right] = 8\pi Q\chi/2 - 4\pi Q\chi = 0\,.$$

Provided eq. (5.20), the solution $U(z)$ to eq. (5.21) is unique up to a constant, and will be the deterministic background potential of the 2D log-REM that we define now.

For this, we denote $u(z)$ the right hand side of eq. (5.21), and perform the *complete–the–square* trick, which is a standard exercise of Gaussian integral (we shall recall it for completeness below). It is also known as Girsanov transform [23], see [22] for rigorous treatment in similar context. Indeed, denoting $\mathcal{O}[\phi]$ a general observable of the GFF ϕ, and using definition of its average, eq. (5.14), we have

$$\begin{aligned}
&\overline{\exp\left[-\int u(z)\phi(z)\mathrm{d}A\right]\mathcal{O}[\phi]} = N_\Sigma^{-1}\int \mathcal{D}\phi \exp\left[\int\left(\frac{1}{16\pi}\phi\Delta\phi - u\phi\right)\mathrm{d}A\right]\mathcal{O}[\phi] \\
=&N_\Sigma^{-1}C_U\int \mathcal{D}\phi \exp\left[\int\left(\frac{1}{16\pi}(\phi-U)\Delta(\phi-U)\right)\mathrm{d}A\right]\mathcal{O}[\phi] \\
=&C_U N_\Sigma^{-1}\int \mathcal{D}\phi \exp\left[\int\left(\frac{1}{16\pi}\phi\Delta\phi\right)\mathrm{d}A\right]\mathcal{O}[\phi+U] = C_U\overline{\mathcal{O}[\phi+U]}\,, \qquad (5.22)
\end{aligned}$$

$$\text{where } C = \exp\left(-\frac{1}{16\pi}\int U\Delta U\mathrm{d}A\right)\,. \qquad (5.23)$$

Note that the constant C is formally infinite in the continuum. Remark that, to resolve this problem, one may carry out the same trick directly for the discrete log-REM, and obtain a constant C which is finite but diverges as one removes the UV cut–off. We will not do this here since fixing the normalization constant is not our goal here.

Now, let us apply this to eq. (5.15). For this, let us rename the second group of vertex operators

$$a_{\ell+i} = q_i b\,,\ w_{i+\ell} = z_i\,,\ i = 1,\dots,m = n-\ell\,. \qquad (5.24)$$

The above trick will transform the partition function (5.9) into

$$Z \overset{\text{def.}}{=} Z_0[\phi \rightsquigarrow \phi + U] = \int e^{-b(\phi+U)}\mathrm{d}A\,. \qquad (5.25)$$

Note also that eq. (5.20) and (5.11) imply

$$s = \sum_{i=1}^m q_i b\,, \qquad (5.26)$$

so we have nicely

$$\begin{aligned}
\left\langle \prod_{j=1}^\ell \mathcal{V}_{a_j}(w_j)\prod_{i=1}^k \mathcal{V}_{q_i b}(z_i)\right\rangle_b &= C'\overline{Z^{-s/b}\prod_{i=1}^m e^{-bq_i(\phi(z_i)+U(z_i))}} \\
=C'\overline{\prod_{i=1}^m [e^{-bq_i(\phi(z_i)+U(z_i))}Z^{-q_i}]} &= C'\overline{\prod_{i=1}^m p_b^{q_i}(z_i)}\,, \qquad (5.27)
\end{aligned}$$

where $C' = C_U \Gamma(s/b) b^{-1} \mu^{-\frac{s}{b}} N_\Sigma$ is another constant, and

$$p_b(z) \overset{\text{def.}}{=} \frac{1}{Z} e^{-b(\phi(z)+U(z))} \tag{5.28}$$

is the Gibbs measure of a thermal particle in the potential $\phi(z)+U(z)$ made of a random 2D GFF and a deterministic logarithmic potential. This equation is valid with further conditions (Seiberg bounds), as we discuss below.

Equation (5.27) indicates, at a continuum level, that LFT correlation functions correspond to the *Gibbs measure statistics* (multi-point correlations of powers of the Gibbs measure) of a log-REM with a composite potential $\phi(z)+U(z)$. This is the core result of the exact mapping established in [11]. We would like to underline the *naturalness* of the link: eq. (5.20) is required by the "charge neutrality condition" imposed by eq. (5.21), and guarantees *at the same time*, *via* eq. (5.26), that the $Z^{-s/b}$ factor has exactly the correct power to allow an interpretation as Gibbs measure.

In this respect, we make an important remark. In order to take into account the free energy distribution, we would need to add another factor $Z^{-t/b} = \exp(tF)$ in the right hand side of eq. (5.27); then, its left hand side would be the correlation function of a field theory defined by the action eq. (5.1) but with $Q \neq b + b^{-1}$. Unfortunately, such a theory is *not* conformal invariant and not exactly solved. Therefore, we are unable to extend fruitfully the current mapping to the include any information on the free energy of the log-REM. Therefore, the exact calculation of the free energy distribution in 2D log-REM remains an open question.

5.2.2 Conditions on the charges

Eq. (5.27) is obtained by continuum manipulations, so it describes correctly the Gibbs measure of the *discrete* log-REM in the thermodynamic/continuum limit only in the high-temperature phase. We have taken care of the normalization of the 2D GFF in eq. (5.13) such that $\overline{\phi(z)\phi(w)} \sim -4 \ln|z-w|$ as $z \to w$ so the critical temperature is $\beta_c = 1$. When $\beta < 1$, the temperature of the log-REM corresponds simply to the parameter b in LFT. When $\beta > 1$, we must combine the 1RSB/freezing results and LFT predictions at $b = 1$ to describe the Gibbs measure of the discrete log-REM. In summary, the following notation will be convenient:

$$b = \begin{cases} \beta\,, & \beta < 1\,, \\ 1\,, & \beta \geq 1\,. \end{cases} \tag{5.29}$$

The condition $\beta = b \leq 1$ is not the only condition for eq. (5.27) to hold:

1. $\sum_i a_i > Q\chi/2$, where a_i are the charges in the LFT correlation. We have already seen it in (5.11) as the condition of convergence of the zero mode integral. In our applications, this is always true, by eq. (5.20), as long as $q_i > 0$ (we will not consider negative powers of Gibbs measure).

2. $a_i < Q/2$ for any of charges, *i.e.*, in eq. (5.27),

$$a_i < Q/2\,,\ i = 1, \ldots, \ell\,, \tag{5.30a}$$
$$q_i < Q/(2b)\,,\ i = 1, \ldots, m\,. \tag{5.30b}$$

For each $a = a_i$, the first condition coincides with the no–binding condition, eq. (2.24). This is the correct interpretation since eq. (5.21) implies that $U(z) \sim -4 \ln |z - w_i|$ near the charge, in agreement with eq. (2.25) ($d = 2$). Therefore eq. (5.30a) is the condition under which none of the singularities of $U(z)$ is too strong to trap the thermal particle at its bottom. Note that eq. (5.30a) and eq. (5.20) imply that for sphere like surfaces, $\chi = 2$, we need a potential $U(z)$ with $\ell \geq 3$ singularities; on the other hand, on the torus, $\chi = 0$, $\ell = 0$ ($U(z) = 0$) is permitted.

For each $q = q_i$, and when $\beta = b \leq 1$, eq. (5.30b) coincides with the phase boundary of the IPR exponent in the annealed ensemble, eq. (4.16). This is not a coincidence, as we will discuss in section 5.4.3. Before that section, we will only consider cases where $\forall i, q_i = 1$, so eq. (5.30b) is always true when $b < 1$.

5.2.3 Infinite plane case, numerical test

We illustrate and check numerically the general result in the special case of infinite plane, which is the one considered in [11] (main text). It is well–known (see for example [20]) that the LFT can be considered on the infinite plane *plus a point*, $\mathbb{C} \cup \{\infty\}$. This surface is closed, topologically identical to the round sphere ($\chi = 2$), but its geometry resembles more the flat Euclidean plane. Its surface element $\mathrm{d}A = \mathrm{d}^2 z$; its curvature $\hat{R} = 8\pi\delta(z - \infty)$ vanishes everywhere but is concentrated at infinity, so that $\int_{\mathbb{C}\cap\infty} \hat{R}\mathrm{d}A = 4\pi\chi$ in agreement with the Gauss–Bonnet theorem eq. (5.10).

The application of the LFT on such a surface to statistical models is problematic. Indeed, the infinite plane case is not yet covered by the rigorous treatments in [22], so presents a new technical challenge and an interesting subject of numerical study. The reason is that the 2D GFF on $\mathbb{C} \cup \{\infty\}$ is ill-defined, and should be considered as the $R \to \infty$ limit of the 2D GFF on a flat domain of linear size R. In practice, we use the periodic boundary condition and the fast Fourier transform, eq. (2.7), to generate it. Note that the resulting covariance is $\overline{\phi(z)\phi(w)} = -4 \ln |z - w|$, see eq. (2.9), and satisfies eq. (5.13) where $V^{-1} = 0$ because the area is infinite. So the 2D GFF is in fact on a *torus* of size R and lattice spacing ϵ. The obvious objection is then: how can the planar/spherical LFT make prediction about this setting?

The reason is the existence of the potential $U(z)$. Recall that it is defined by a set of charges $(a_i, w_i), i = 1, \ldots, \ell$, such that $\sum_i a_i = Q$ *via* eq. (5.21). The Seiberg bounds eq. (5.30a) imply $\ell \geq 3$. We take the minimum $\ell = 3$, and set $(w_1, w_2, w_3) = (0, 1, \infty)$. Then eq. (5.21) is solved by

$$U(z) = 4a_1 \ln |z| + 4a_2 \ln |z - 1| \ , \tag{5.31}$$

up to a constant. The Seiberg bound eq. (5.30a) for the charge at infinity, $a_3 < Q/2$, becomes equivalent to $a_1 + a_2 > Q/2$ because $a_3 = Q - a_1 - a_2$, by eq. (5.20). Since the point is at infinite, the Seiberg bound acquires another interpretation: it guarantees that thermal particle does not *escape to* $w_3 = \infty$.

A simple way to understand this is to proceed by analogy with the analysis of the Gaussian model in section **??** (see the paragraph before eq. (**??**)). Recall that the free energy of the log-REM with potential $\phi(z)$ alone (without $U(z)$) has extensive free energy $\mathcal{F} = -Q \ln M = -2Q \ln R + 2 \ln \epsilon$ ($M = (R/\epsilon)^2$ is the size of the log-REM). Now, when

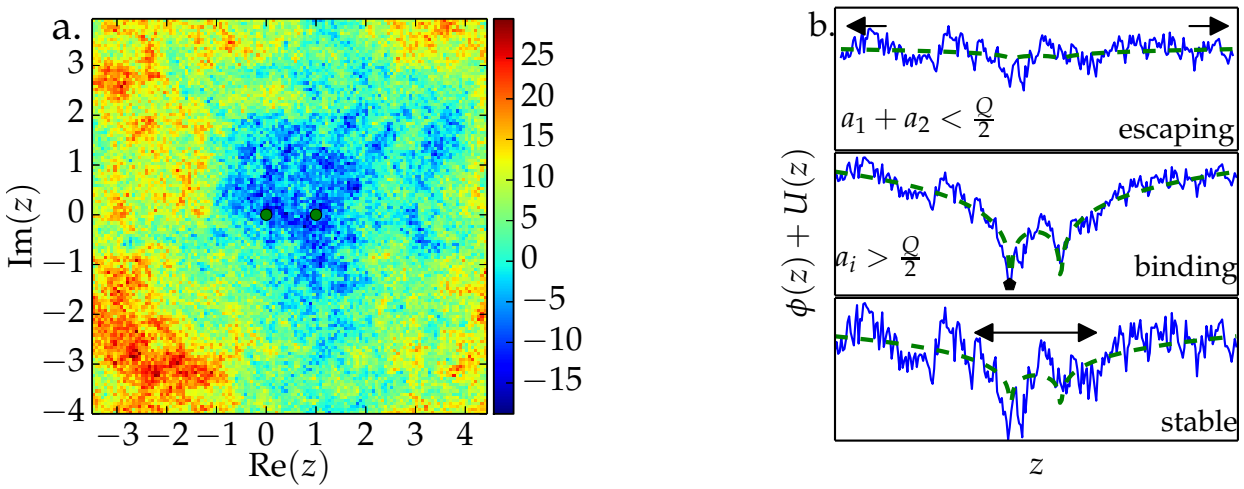

Figure 9. Taken from [11]. a. Colour plot of a sample of 2D GFF plus the log confining potential $U(z)$ (5.31) with $a_{1,2} = .8, .6$. The two singularities $z = 0, 1$ are indicated by green dots. The domain has lattice spacing $\epsilon = 2^{-5}$ and size $R = 8$, with periodic boundary condition. b. Top: When the potential is too shallow the particle escapes to ∞, and the Gibbs measure vanishes as $R \to \infty$. Middle: When the potential is too deep, the Gibbs measure becomes a δ peak as $\epsilon \to 0$. Bottom: When all the Seiberg bounds are satisfied, the extent of the central region is stable as $R \to \infty, \epsilon \to 0$ and the limiting Gibbs measure can be compared to planar LFT.

$U(z)$ is added, the free energy cost for a particle to escape to R is $F(R) = \mathcal{F} + U(R) \approx -2Q \ln(R) + 4(a_1 + a_2) \ln R + c = 4(a_1 + a_2 - Q/2) \ln R + c$ where c is R-independent. So $a_1 + a_2 > Q/2$ is equivalent to $F(R) \to +\infty$ as $R \to \infty$, *i.e.*, escaping is unfavourable. Thus, as we anticipated in section **??**, the log-REM with potential $\phi(z) + U(z)$ considered here is a *IR divergent log-REM*. Its free energy distribution suffers from the same problems as the Gaussian model; yet, its Gibbs measure can be still studied.

Thus, when the $a_1 < Q/2, a_2 < Q/2$, but $a_1 + a_2 > Q/2$, the particle in the potential $\phi(z) + U(z)$ is neither trapped at 0 or 1 nor escaping to infinity, and its Gibbs measure is expected to be stable in the limit $R \to \infty$ (as well as $\epsilon \to 0$). Since the scale R becomes irrelevant, the detail of IR regularization (*i.e.* the periodic boundary condition) is irrelevant, and the LFT on $\mathbb{C} \cup \{\infty\}$ is suited to describe it. The simplest prediction made by eq. (5.19) relates the disorder–averaged Gibbs measure to a 4 point function of LFT on $\mathbb{C} \cup \{\infty\}$:

$$\overline{p_\beta(z)} \propto \langle \mathcal{V}_{a_1}(0) \mathcal{V}_{a_2}(1) \mathcal{V}_b(z) \mathcal{V}_{a_3}(\infty) \rangle_b \ , \ a_3 = Q - a_1 - a_2 \, . \tag{5.32}$$

Although eq. (5.19) is limited to the $\beta < 1$ phase, we have seen in eq. (**??**) that $\overline{p_\beta(z)}$ becomes temperature–independent in the $\beta > 1$ phase. So eq. (5.32) still holds in that phase, thanks to the notation eq. (5.29).

Equation (5.32) was tested numerically in [11]. Its left hand side was measured on large scale simulations of 2D GFF (see Figure 10 for parameters). The right hand side can be calculated using the conformal bootstrap solution of LFT, in terms of an involved analytical expression, as will be described in the next section. Fortunately, the code-base

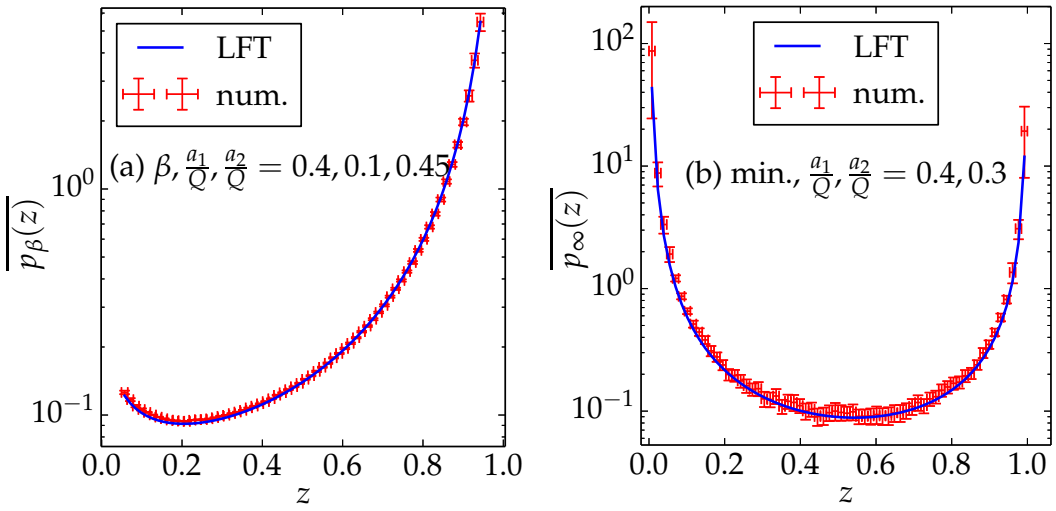

Figure 10. Taken from [11]. Test of (5.32) on the segment $z \in [0,1]$. (a) High-T regime ($\beta = .4, a_1/Q = .1, a_2/Q = .45$). (b) Minimum position distribution versus LFT with $b = 1$ ($a_1/Q = .4, a_2/Q = .3$). The 2D GFF is generated on a square lattice with size $R = 2^3$ and lattice spacing $\epsilon = 2^{-9}$, with periodic boundary condition, using eq. (2.7). There are 5×10^6 independent samples for each measure.

[24] is a powerful and accessible toolbox for numerical computation of LFT four–point functions. For the present application, we extend the code to take into account discrete fusions between vertex operators of type $\mathcal{V}_a$, $a \in (0, Q/2)$ (this point will be discussed in more detail in the next section 5.3), and calculates easily the right hand side of (5.32) with 10^{-5} precision, which is enough for the present application . The left hand side of (5.32) is measured on extensive simulations of discrete 2D GFF. The results are reported in Figure 10. In each test, the values of both sides of (5.32) for $x = z \in (0,1)$ are considered; the only unknown parameter is the global normalisation factor, which is fixed by matching the empirical mean of the logarithms. The results confirm well the prediction eq. (5.32).

5.3 Conformal Bootstrap and OPE

In the conformal bootstrap solution of LFT (Sylvain lectures) we have the following expression for the 4–point function of LFT

$$\begin{aligned} &\langle \mathcal{V}_{a_1}(0)\mathcal{V}_{a_4}(z)\mathcal{V}_{a_2}(1)\mathcal{V}_{a_3}(\infty)\rangle_b \\ &= \int_{\mathcal{A}_L} C^{\mathrm{DOZZ}}(a_1, a_4, a) C^{\mathrm{DOZZ}}(Q-a, a_2, a_3) |\mathcal{F}_{\Delta_a}(\{a_i\}, z)|^2 \, |\mathrm{d}a| \;, \forall a_i \in \mathcal{A}_L \end{aligned} \tag{5.33}$$

Let us explain the notations of the right hand side:

- The integral is over the *spectrum* of LFT:

$$\mathcal{A}_L = \frac{Q}{2} + \mathbf{i}\mathbb{R} = \left\{ \frac{Q}{2} + \mathbf{i}P : P \in \mathbb{R} \right\} . \tag{5.34}$$

- C^{DOZZ} is the DOZZ *structure constants* of LFT (the two groups of authors found them independently [4, 25]). We will discuss them in more detail below.

- Δ_a is the *conformal dimension* of the field $\mathcal{V}_a(z)$. In LFT,

$$\Delta_a = a(Q-a)\,. \tag{5.35}$$

  We note that a general CFT is determined completely by its spectrum, the conformal dimensions, and its structure constants.

- $\mathcal{F}_{\Delta_a}(\{a_i\}, z)$ is the *conformal block*. It is a function of z, and the five conformal dimensions $\Delta_a, \Delta_{a_1}, \ldots, \Delta_{a_4}$. It is known analytically, and efficiently calculated by the code–base [24]. It is universal to all 2D CFT, *i.e.*, the same function would appear if we consider eq. (5.33) for another CFT.

5.3.1 The DOZZ structure constant

The DOZZ structure constants are known to be:

$$C^{\mathrm{DOZZ}}(a_1,a_2,a_3) = \\ \frac{\left[b^{\frac{2}{b}-2b}\mu\right]^{Q-a_1-a_2-a_3}\prod_{i=1}^{3}\Upsilon_b(2a_i)}{\Upsilon_b(\sum_{i=1}^{3}a_i-Q)\Upsilon_b(a_1+a_2-a_3)\Upsilon_b(a_1-a_2+a_3)\Upsilon_b(-a_1+a_2+a_3)}\,. \tag{5.36}$$

Here, the only analytical property we need is that: $\Upsilon_b(z)$ is analytic on $\mathbb{C}$, with infinitely many simple zeros:

$$\Upsilon_b(z)=0 \Leftrightarrow z\in\left\{-bm-b^{-1}n : m,n=0,1,2\ldots\right\} \\ \bigcup\left\{Q+bm+b^{-1}n : m,n=0,1,2\ldots\right\} \tag{5.37}$$

Observe they are organized into two *lattices*: one ranging from 0 to $-\infty$, the other from Q to $+\infty$, and the two related by the symmetry $a\mapsto Q-a$.

An important consequence of eq. (5.37) is that, the DOZZ formula eq. (5.36) has a simple zero at $a_3 = Q/2$ (coming from $\Upsilon_b(2a_3)$ in the numerator)

$$C^{\mathrm{DOZZ}}(a_1,a_2,Q/2+p) = c_1 p + O(p^2)\,,\ |p| << 1\,. \tag{5.38}$$

where c_1 is some factor, for *generic* a_1 and a_2, *i.e.*, when all the other DOZZ functions do not vanish. When they do, the zero might be cancelled by one in the denominator, or become of higher order.

5.3.2 Discrete terms

The integral eq. (5.33) is a contour integral of a meromorphic function of a. It has many poles which come from the zeros of the Υ's in the denominator of the DOZZ formula eq. (5.36), so their positions depend on a_i. Now, when a_i moves smoothly away from $\mathcal{A}_L$ to their positions in eq. (5.32), some poles may cross the integral contour $\mathcal{A}_L$. To analytically continue the contour integral, the contour needs to be deformed to prevent the pole from crossing it, in the way indicated by Figure 12. Then, by Cauchy's theorem, the new contour integral can be evaluated as the integral along the old contour, plus a *discrete term*:

$$D_p = \pm 2\pi\ \mathrm{Res}_{a\to p}\left[C^{\mathrm{DOZZ}}(a,a_1,a_4)C^{\mathrm{DOZZ}}(Q-a,a_2,a_3)\right]\left|\mathcal{F}_{\Delta_a}(\{a_i\},z)\right|^2\,, \tag{5.39}$$

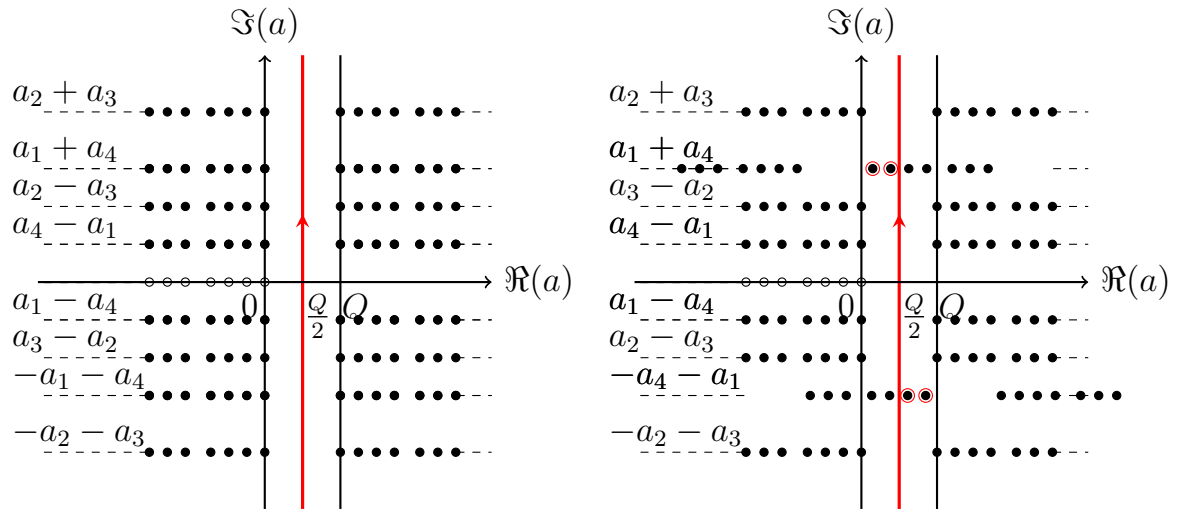

Figure 11. *Left*: The poles of the integrand in (5.33) in the complex plane of a when $\Re(a_i) = \frac{Q}{2}$, $i = 1, .., 4$. The filled and empty dots indicate respectively the position of the poles of the structure constants and of the conformal blocks $(-L/2)$. The red line is the integration contour $\mathcal{A}_L = Q/2 + \mathbf{i}\mathbb{R}$. *Right*: The same plot, with a parameter set such that $\Re(a_2) = \Re(a_3) = Q/2$ but $\Re(a_1) = \Re(a_4) < Q/2$, and $\Re(a_1 + a_4) < Q/2$. The poles that have crossed the contour are marked by red circles.

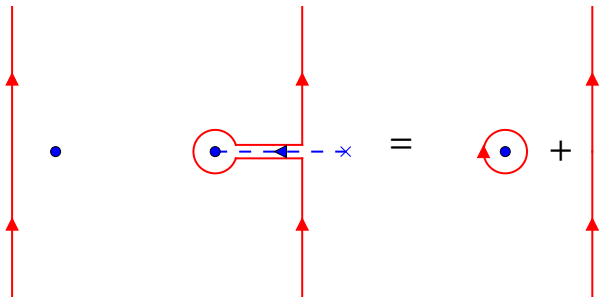

Figure 12. An illustration of the deformation of a contour integral. *Left*: an integral contour is drawn in red line (with arrow) and a pole at its initial condition is drawn as a blue dot. *Middle*: the pole moves smoothly to the left of the contour. In order to prevent crossing, the contour is deformed. *Right*: Applying Cauchy's theorem to the previous contour reduces it into the sum of the contribution of a residue (*discrete term*) and that of a continuous integral.

Therefore, the correctly generalized version of eq. (5.33) is

$$\langle \mathcal{V}_{a_1}(0)\mathcal{V}_{a_4}(z)\mathcal{V}_{a_2}(1)\mathcal{V}_{a_3}(\infty)\rangle = 2\sum_{p\in P_-^{14}} D_p + (14 \rightsquigarrow 23) + \int_{\mathcal{A}_L} C^{\mathrm{DOZZ}}(a_1,a_4,a)C^{\mathrm{DOZZ}}(Q-a,a_2,a_3)|\mathcal{F}_{\Delta_a}(\{a_i\},z)|^2\,|\mathrm{d}a|\ . \tag{5.40}$$

5.3.3 Asymptotic behaviour (OPE)

We have to distinguish three cases, illustrated in Figure 13:

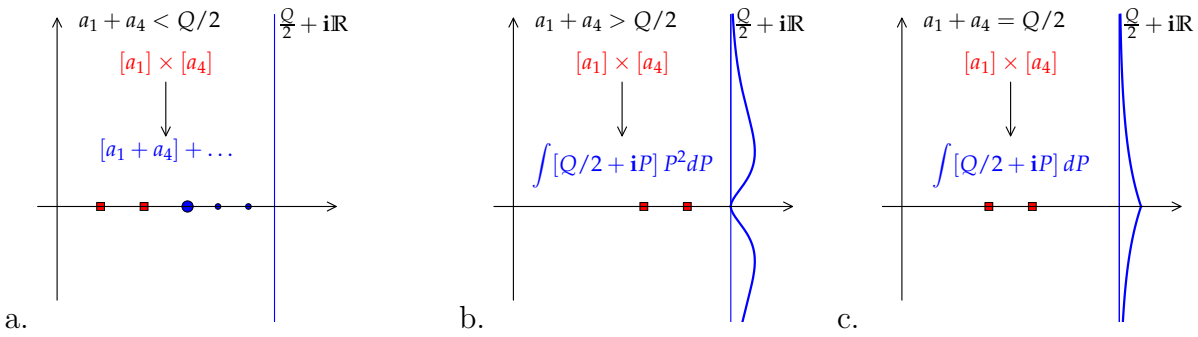

Figure 13. Illustrations of the three cases of OPE. In each case the (upper-half) complex plane of charge values are drawn. Red squares indicate the charges a_1 and a_4. The charge(s) dominating the OPE is written in blue. The Blue dots indicate the positions of poles included in (5.40); the largest one dominates the OPE. The blue straight line is the LFT spectrum. The blue thick curves are cartoons of the value of the integrand in eq. (5.33), highlighting their behaviour near $a = Q/2$.

(a) $a_1 + a_4 < \frac{Q}{2}$ (pole crossing). The smallest scaling dimension is given by the discrete term $a = a_1 + a_4 \in P_-$. So (**??**) implies

$$\langle \mathcal{V}_{a_1}(0)\mathcal{V}_{a_4}(z)\mathcal{V}_{a_2}(1)\mathcal{V}_{a_3}(\infty)\rangle \underset{z\to 0}{\sim} |z|^{-2\delta_0}\,, \tag{5.41}$$
$$\delta_0 = \Delta_{a_1} + \Delta_{a_4} - \Delta_{a_1+a_4} = 2a_1a_4\,.$$

(b) $a_1 + a_4 > \frac{Q}{2}$ (no pole crossing). There are no discrete terms, and the smallest dimension is given by $a = Q/2$ in the continuous integral. Now, recalling that the $Q/2$ belongs to the continuous spectrum ($Q/2+\mathbf{i}\mathbb{R}$), we need to consider the vicinity of $Q/2$. Moreover, $C^{\mathrm{DOZZ}}(a, a_1, a_4)$ and $C^{\mathrm{DOZZ}}(Q - a, a_2, a_3)$ have a simple zero at $a = Q/2$ (eq. (5.38)), so eq. (**??**) and (5.40) imply

$$\langle \mathcal{V}_{a_1}(0)\mathcal{V}_{a_4}(z)\mathcal{V}_{a_2}(1)\mathcal{V}_{a_3}(\infty)\rangle \underset{z\to 0}{\sim} \int_{\mathbb{R}} |z|^{-2\delta_1-2P^2} P^2\,\mathrm{d}P\,, \tag{5.42}$$
$$\sim |z|^{-2\delta_1} \ln^{-\frac{3}{2}} |1/z|\,,\ \delta_1 = \Delta_{a_1} + \Delta_{a_4} - \Delta_{Q/2}\,. \tag{5.43}$$

(c) $a_1 + a_4 = \frac{Q}{2}$ (marginal case). This case is similar to the above one, except that $C^{DOZZ}(a, a_1, a_4)C^{DOZZ}(Q - a, a_2, a_3)$ does not vanish at $a = Q/2$, so we have

$$\langle \mathcal{V}_{a_1}(0)\mathcal{V}_{a_4}(z)\mathcal{V}_{a_2}(1)\mathcal{V}_{a_3}(\infty)\rangle \underset{z\to 0}{\sim} \int_{\mathbb{R}} |z|^{-2\delta_0-2P^2}\mathrm{d}P \sim |z|^{-2\delta_0} \ln^{-\frac{1}{2}} |1/z|\,. \tag{5.44}$$

This case can also be understood as the pair of dominant poles in case (a) merging at $Q/2$ and compensating the double zero of case (b).

In summary, the results of this section can be summarized in the following:

$$\langle \mathcal{V}_{a_1}(z)\mathcal{V}_{a_2}(0)\dots\rangle_b \overset{z\to 0}{\sim} \begin{cases} |z|^{-2\eta} \ln^{-\frac{3}{2}} |1/z| & a_1 + a_2 > Q/2\,, \\ |z|^{-4a_1a_2} \ln^{-\frac{1}{2}} |1/z| & a_1 + a_2 = Q/2\,, \\ |z|^{-4a_1a_2} & a_1 + a_2 < Q/2\,. \end{cases} \tag{5.45}$$

$$\eta \overset{\text{def.}}{=} \Delta_{a_1} + \Delta_{a_2} - \Delta_{\frac{Q}{2}}\,,\ \Delta_a = a(Q - a)\,. \tag{5.46}$$

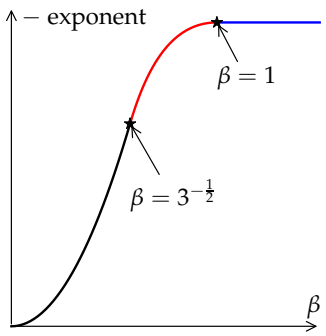

Figure 14. A plot of the exponent of $|z|$ in eq. (5.47), as a function of the temperature.

5.4 Application to logREMs

5.4.1 Two thermal particles

Let us now consider two independent thermal particles in a same random potential. To characterize their attraction, we can consider the joint probability distribution of their positions, given by the two point correlation function of the Gibbs measure $\overline{p_\beta(w)p_\beta(w+z)}$, and focus on its asymptotic behaviour as $z \to 0$. The results read as follows:

$$\overline{p_\beta(w)p_\beta(z+w)} \overset{z\to 0}{\sim} \begin{cases} |z|^{-4\beta^2} & \beta < 3^{-\frac{1}{2}} \\ |z|^{-4/3} \ln^{-\frac{1}{2}} |1/z| & \beta = 3^{-\frac{1}{2}} \\ |z|^{-3+\frac{\beta^2+\beta^{-2}}{2}} \ln^{-\frac{3}{2}} |1/z| & \beta \in (3^{-\frac{1}{2}}, 1] \\ c'\beta^{-1} |z|^{-2} \ln^{-\frac{3}{2}} |1/z| + (1-\beta^{-1})\delta(z) & \beta > 1\,. \end{cases} \tag{5.47}$$

where c' is an unknown constant (which will depend on other details of the log-REM). Note that the β dependence of the exponent has two non-analyticities (see Figure 14). The one at $\beta = 1$ comes from the freezing transition. The other one is inside the in the $\beta < 1$ phase, but is associated with the logarithmic corrections reminiscent of the freezing transition. Its value is also quite mysterious: we shall interpret in terms of multi–fractality in section 5.4.3.

We can also combine eq. (5.47) and eq. (**??**) to obtain an asymptotic behaviour of the joint distribution $P(z_1, z_2)$ of the first and second minima positions:

$$P(z_1, z_2) \sim |z_1 - z_2|^{-2} \ln^{-\frac{3}{2}} |1/(z_1 - z_2)|\,. \tag{5.48}$$

This holds for $1 \gg |z_1 - z_2| \gg \epsilon$ (ϵ is the lattice spacing), while the δ in (5.47) takes over as $|z| \sim \epsilon$).

5.4.2 Finite–size correction to overlap distribution

The previous result eq. (5.47) can be applied to a translation invariant setting, *i.e.*, a torus of size $R = 1$ (the thermodynamic limit is obtained by letting the lattice spacing $\epsilon \to 0$), and with $U(z) = 0$. Then, eq. (5.47) is related to the distribution of the (squared) distance $r^2 = |z|^2$ between the two thermal particles. Denoting $P(r^2)$ the PDF, we have $\mathrm{d}P = P(r^2)\mathrm{d}r^2 = \overline{p_\beta(w)p_\beta(r+w)}2\pi r\mathrm{d}r$, so

$$P(r^2) = \pi\overline{p_\beta(w)p_\beta(r+w)}\,, \tag{5.49}$$

where $P(r^2)$ is the PDF of r^2.

In log-REM, there is another notion of the distance, the overlap q. Its relation with the Euclidean distance is given by eq. (**??**). With $d = 2$ and $R = 1$, it implies

$$\mathsf{q} = -\ln(r^2)/t\,,\; t = \ln M = \ln(1/\epsilon^2)\,. \tag{5.50}$$

Recall also that in the thermodynamic $t \to \infty$ limit, the limit distribution of q is known to be (see eq. (4.7))

$$P(\mathsf{q}) \to \begin{cases} \delta(\mathsf{q}) & \beta < 1 \\ \beta^{-1}\delta(\mathsf{q}) + (1-\beta^{-1})\delta(1-\mathsf{q}) & \beta > 1 \end{cases} \tag{5.51}$$

Now, equations eq. (5.50) and eq. (5.49) applied to LFT prediction eq. (5.47), give us *finite–size corrections* to eq. (5.51):

$$\begin{aligned} P(\mathsf{q}) &= \frac{\mathrm{d}r^2}{\mathrm{d}\mathsf{q}}\overline{\pi p_\beta(w)p_\beta(r+w)} = e^{\mathsf{q}t}\overline{\pi p_\beta(w)p_\beta(r+w)} \\ &\sim \begin{cases} e^{(2\beta^2-1)t\mathsf{q}}\, t & \beta < 3^{-\frac{1}{2}} \\ e^{-\mathsf{q}t/3}\,\mathsf{q}^{-\frac{1}{2}}t^{\frac{1}{2}} & \beta = 3^{-\frac{1}{2}} \\ e^{-(\beta-\beta^{-1})^2 t\mathsf{q}/4}\, t^{-\frac{1}{2}}\mathsf{q}^{-\frac{3}{2}} & \beta \in (3^{-\frac{1}{2}}, 1) \\ t^{-\frac{1}{2}}\mathsf{q}^{-\frac{3}{2}} & \beta \geq 1, q << 1\,. \end{cases} \end{aligned} \tag{5.52}$$

In the last case $\beta > 1$, we do not know how to transform the Dirac peak $\delta(z)$ in eq. (5.47) to the variable q; qualitatively, a probability mass of $1 - \beta^{-1}$ must be attributed to the regime $\mathsf{q} \sim 1$ in the $t \to \infty$ limit. So the formula given in eq. (5.52) can be only right for $\mathsf{q} << 1$. In the other cases, the expressions in eq. (5.52) are consistent with eq. (5.51) at $\mathsf{q} \sim 1$, so we believe that they are correct for all q.

Note that, while eq. (5.47) is a prediction for a log-REM in 2D, eq. (5.52) makes sense for *any log-REM*. Motivated by the universality of log-REM, we conjecture that eq. (5.52) holds for general log-REM. We do not know yet a complete argument supporting this conjecture, say, using the replica approach. More precisely, we know how to recover the leading behaviours $e^{-c\mathsf{q}}$ in eq. (5.52), using 1RSB, by generalizing the arguments of [26]; the difficulty lies in recovering the log–corrections.

However, a confirmation of our conjecture comes from a recent result [27], which studies the same quantity on the directed polymer on the Cayley tree model. Their results concern only the $\beta > 1$ phase and the critical point $\beta = 1$, but is valid for all $\mathsf{q} \in (0, 1)$. We quote them below (eq. 6 and 7, *op. cit.*, with $\beta_c = 1$, $v(\beta) = -\beta - \beta^{-1}$, $v''(\beta_c) = 2$):

$$P(\mathsf{q}) \sim t^{-\frac{1}{2}}\mathsf{q}^{-\frac{3}{2}}\frac{1}{\beta\sqrt{4\pi}}(1-\mathsf{q})^\eta\,,\; \eta = \begin{cases} \frac{1}{2} & \beta = 1 \\ \frac{3}{2} & \beta > 1\,. \end{cases} \tag{5.53}$$

So it agrees with eq. (5.52) while giving more precision on the pre–factor.

5.4.3 Multi–fractality revisited

We observed that eq. (5.47) has a non–analyticity at $\beta = 1/\sqrt{3}$. What transition does it correspond to? In [11], we claimed that the answer is the termination point transition,

discussed in section 4. Here we will explain this claim, and give an argument for the last equation in the main text of [11]. Throughout this section, we will assume $\beta = b < 1$.

Recall that if $p_{\beta,j}, j = 1, \dots, M$ is the Gibbs measure of a discrete log-REM of size M, the IPR in the *annealed ensemble* is given by eq. (4.16):

$$\overline{P_q} = M\overline{p_{\beta,j}^q} \sim M^{-\tau_q}\,,\ \tau_q = \begin{cases} q\beta\,(Q - q\beta) - 1\,, & q < Q/(2\beta)\,, \\ Q^2/4 - 1\,, & q \geq Q/(2\beta)\,, \end{cases} \tag{5.54}$$

where in the first equation, we assume that the log-REM is homogeneous. Our goal is to give arguments for the *logarithmic correction* to the leading behaviour, announced in [11]:

$$\overline{P_q} \overset{\beta<1}{\sim} \begin{cases} M^{-\tau_q} & q\beta < \frac{Q}{2} \\ M^{-\tau_q} \ln^{\frac{1}{2}} M & q\beta = \frac{Q}{2} \\ M^{-\tau_q} \ln^{\frac{3}{2}} M & q\beta > \frac{Q}{2} \end{cases}. \tag{5.55}$$

We will use LFT to argue for this in the 2D context; extension to general log-REM can be argued again based on the their universality. Before proceeding, we note that the analogue of eq. (5.55) for the uncorrelated REM is known [26]. The exponents τ_q is the same, but the corrections are different: there is only a $\frac{1}{2}\ln\ln M$ correction when $q\beta > Q/2$. For the log-REM, the logarithmic corrections in the *typical* ensemble (see section 4) were calculated much earlier in Sec. VI.B in [9], without using LFT.

When $q\beta < Q/2$, the vertex operator $\mathcal{V}_{q\beta}$ satisfies the Seiberg bound eq. (5.30b), and can be used to describe the power of the Gibbs measure $p_{\beta,j}^q$. Since the latter is on the discrete lattice, the corresponding operator is the *bare* one, and its one point function is (in general CFT) given by

$$\langle \mathcal{V}_a \rangle_b \sim M^{-\Delta_a}\,, \tag{5.56}$$

where $\Delta_a = a(Q - a)$ (eq. (5.35)) is the conformal dimension. Therefore,

$$\overline{P_q} = M\overline{p_{j,\beta}} = M\,\langle \mathcal{V}_{q\beta} \rangle_b \sim M^{-\tau_q}\,,\ \tau_q = \Delta_{q\beta} - 1\,, \tag{5.57}$$

giving the first case. Note that the matching between Δ_a and the IPR exponent in log-REM was observed at least as early as from the pioneering work [3].

When $q\beta \geq Q/2$, $\mathcal{V}_{q\beta}$ can no longer represent $p_{\beta,j}^q$. To proceed, we split $q = q_1 + q_2 + \dots + q_n$ such that $q_i\beta < Q/2$, and represent $p_{\beta,j}^q$ by a product of vertex operators $\mathcal{V}_{q_1\beta} \dots \mathcal{V}_{q_n\beta}$, evaluated at close but not identical points. Then we apply the LFT fusion rules ([28], Exercise 3.3) to them. Let us explain with a case where $n = 2$ suffices. The relevant LFT fusion rule reads (see also Figure 13):

$$\mathcal{V}_{a_1}\mathcal{V}_{a_2} \sim \begin{cases} \mathcal{V}_{a_1+a_2} + \dots & a_1 + a_2 < Q/2\,, \\ \int \mathcal{V}_{\frac{Q}{2}+\mathbf{i}P}\mathrm{d}P & a_1 + a_2 = Q/2\,,\ a_1, a_2 \in (0, Q/2)\,. \\ \int \mathcal{V}_{\frac{Q}{2}+\mathbf{i}P} P^2 \mathrm{d}P & a_1 + a_2 > Q/2\,, \end{cases} \tag{5.58}$$

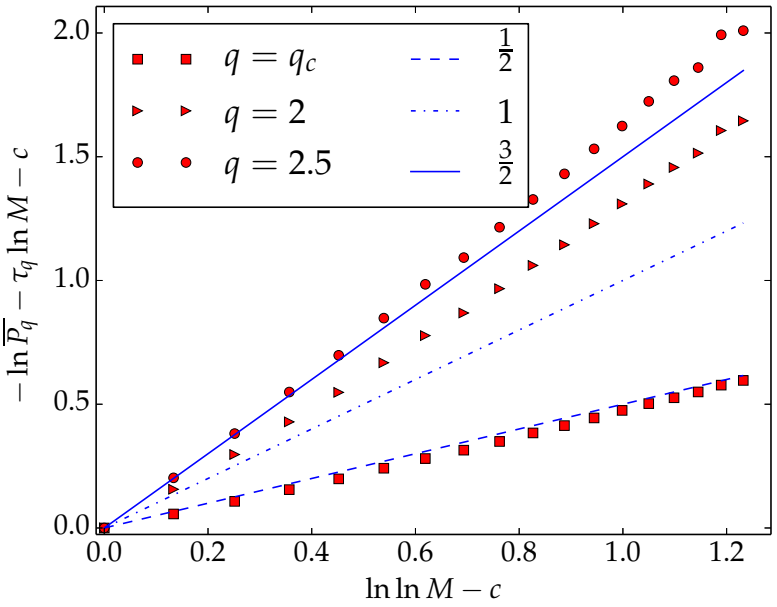

Figure 15. Numerical measure the annealed IPR with $\beta = .75$, with $q = q_c = (Q/2\beta), 2$ and $q = 2.5$, in the circular model, with $M = 2^7, \ldots, 2^{24}$. We take the logarithm, remove the leading order in eq. (5.55) and compare the resulting correction to $\frac{3}{2} \ln \ln M$, $\ln \ln M$, $\frac{1}{2} \ln \ln M$ (which are the slopes of the straight lines through origin). For better comparison, we translate each data set so that its first point is at the origin.

Both integrals are performed on $(-\epsilon, \epsilon)$, a small interval around $P = 0$. Combined with eq. (5.56), we have, when $q\beta > Q/2$,

$$\begin{aligned} \overline{P_q} = M\overline{p_{j,a}} \sim M \left\langle \mathcal{V}_{q_1\beta} \mathcal{V}_{q_2\beta} \right\rangle \sim M \int \left\langle \mathcal{V}_{\frac{Q}{2}+\mathrm{i}P} \right\rangle P^2 \mathrm{d}P \\ \sim M \int M^{-\Delta_{\frac{Q}{2}+\mathrm{i}P}} P^2 \mathrm{d}P = M^{1-Q^2/4} \int M^{-P^2} P^2 \mathrm{d}P = M^{1-Q^2/4} \ln^{-\frac{3}{2}} M \,, \end{aligned} \tag{5.59}$$

which is the third case of eq. (5.55). The second case is completely similar: the $\ln^{-\frac{1}{2}} M$ correction comes from $\int M^{-P^2} \mathrm{d}P$. Remark also that if $a_1 + a_2 < Q/2$, the first fusion rule would lead to no logarithmic correction, in agreement with eq. (5.55). Note that the end result does not depend on how we split qa, because of eq. (5.58). For general $n > 2$, the above procedure can be repeated (by using other fusion rules of *op. cit.*); we can still show that the end result is eq. (5.55), regardless of how we split qa.

To further support the claim eq. (5.55), we have performed numerical measures of eq. (5.55) on the circular model, which is a *1D* log-REM. So strictly speaking, the derivation of this section does not directly apply. However, our preliminary result, as shown in Figure 15, gives encouraging support to eq. (5.55) as a *general* log-REM prediction.

To conclude this section, we emphasize that the above discussion is limited to the $\beta < 1$ phase. Indeed, it is clear that eq. (5.55) cannot hold in the $\beta > 1$ phase, since for $q = 1$, we would be in the termination point phase, but the log–correction cannot be present because $\overline{P_1} = 1$ by definition.

References

[1] A. Kupiainen, "Liouville Conformal Field Theory: A ProbabilisticApproach."

[2] B. Duplantier, R. Rhodes, S. Sheffield and V. Vargas, *Log-correlated Gaussian fields: an overview*, *arXiv:1407.5605* (2014) .

[3] I. I. Kogan, C. Mudry and A. M. Tsvelik, *Liouville theory as a model for prelocalized states in disordered conductors*, *Physical Review Letters* **77** (Jul, 1996) 707–710.

[4] A. Zamolodchikov and A. Zamolodchikov, *Conformal bootstrap in liouville field theory*, *Nuclear Physics B* **477** (1996) 577–605.

[5] J. Teschner, *Liouville theory revisited*, *Classical and Quantum Gravity* **18** (2001) R153.

[6] J. Teschner and G. Vartanov, *Supersymmetric gauge theories, quantization of $\mathcal{M}_{\text{flat}}$, and conformal field theory*, *Advances in Theoretical and Mathematical Physics* **19** (2015) .

[7] A. A. Belavin and A. B. Zamolodchikov, *Integrals over moduli spaces, ground ring, and four-point function in minimal liouville gravity*, *Theoretical and mathematical physics* **147** (2006) 729–754.

[8] K. Aleshkin and V. Belavin, *On the construction of the correlation numbers in minimal liouville gravity*, *Journal of High Energy Physics* **2016** (2016) 142.

[9] D. Carpentier and P. Le Doussal, *Glass transition of a particle in a random potential, front selection in nonlinear renormalization group, and entropic phenomena in liouville and sinh-gordon models*, *Physical Review E* **63** (2001) 026110.

[10] B. Derrida, *Random-energy model: Limit of a family of disordered models*, *Physical Review Letters* **45** (1980) 79.

[11] X. Cao, P. Le Doussal, A. Rosso and R. Santachiara, *Liouville field theory and log-correlated Random Energy Models*, *Physical Review Letters* **118** (2017) 090601.

[12] X. Cao, Y. V. Fyodorov and P. Le Doussal, *One step replica symmetry breaking and extreme order statistics of logarithmic REMs*, *SciPost Physics* **1** (2016) 011.

[13] F. J. Dyson, *Statistical theory of the energy levels of complex systems. i*, *Journal of Mathematical Physics* **3** (1962) 140–156.

[14] I. Dumitriu and A. Edelman, *Matrix models for beta ensembles*, *Journal of Mathematical Physics* **43** (2002) 5830–5847.

[15] Y. V. Fyodorov, P. Le Doussal and A. Rosso, *Freezing transition in decaying burgers turbulence and random matrix dualities*, *EPL (Europhysics Letters)* **90** (2010) 60004.

[16] Y. V. Fyodorov and P. Le Doussal, *Moments of the position of the maximum for gue characteristic polynomials and for log-correlated gaussian processes*, *Journal of Statistical Physics* **164** (2016) 190–240.

[17] V. S. Dotsenko and V. A. Fateev, *Conformal algebra and multipoint correlation functions in 2d statistical models*, *Nuclear Physics B* **240** (1984) 312–348.

[18] B. Duplantier and S. Sheffield, *Duality and the knizhnik-polyakov-zamolodchikov relation in liouville quantum gravity*, *Physical Review Letters* **102** (Apr, 2009) 150603.

[19] C. Chamon, C. Mudry and X.-G. Wen, *Localization in two dimensions, gaussian field theories, and multifractality*, *Physical review letters* **77** (1996) 4194.

[20] A. Zamolodchikov and A. Zamolodchikov, *Lectures on Liouville theory and matrix models*, 2007.

[21] M. Goulian and M. Li, *Correlation functions in liouville theory*, *Physical Review Letters* **66** (1991) 2051.

[22] F. David, A. Kupiainen, R. Rhodes and V. Vargas, *Liouville quantum gravity on the riemann sphere*, *Communications in Mathematical Physics* **342** (2016) 869–907.

[23] I. V. Girsanov, *On transforming a certain class of stochastic processes by absolutely continuous substitution of measures*, *Theory of Probability & Its Applications* **5** (1960) 285–301.

[24] S. Ribaut and R. Santachiara, "Bootstrap 2D Python."

[25] H. Dorn and H.-J. Otto, *Two-and three-point functions in liouville theory*, *Nuclear Physics B* **429** (1994) 375–388.

[26] Y. V. Fyodorov, *Pre-freezing of multifractal exponents in random energy models with a logarithmically correlated potential*, *Journal of Statistical Mechanics: Theory and Experiment* **2009** (2009) P07022.

[27] Derrida, Bernard and Mottishaw, Peter, *On the genealogy of branching random walks and of directed polymers*, *EPL* **115** (2016) 40005.

[28] S. Ribault, *Conformal field theory on the plane*, *arXiv:1406.4290* (2014) .